ELSEVIER Applied Mathematics and Computation 121 (2001) 219–259

APPLIED MATHEMATICS AND COMPUTATION

www.elsevier.com/locate/amc

# An efficient and stable approach for computation of Lyapunov characteristic exponents of continuous dynamical systems

Firdaus E. Udwadia [a,*,1], Hubertus F. von Bremen [b]

[a] *Departments of Civil Engineering, Mechanical Engineering, Mathematics, and Business, University of Southern California, Los Angeles, CA 90089-1453, USA*

[b] *Department of Mechanical Engineering, University of Southern California, Los Angeles, CA 90089-1453, USA*

**Abstract**

This paper proposes a new approach for computing the Lyapunov Characteristic Exponents (LCEs) for continuous dynamical systems in an efficient and numerically stable fashion. The method is adapted to systems with small dimensions. Numerical examples illustrating the accuracy of method are presented. 

*Keywords:* Computation of Lyapunov characteristic exponents; Continuous dynamical systems; Intrinsic preservation of orthogonality; Low order systems

## 1. Introduction

Lyapunov characteristic exponents (LCEs) were introduced by Lyapunov [1] when studying the stability of non-stationary solutions of ordinary differential equations. Presently LCEs play a key role in the study of non-linear dynamical systems. The LCEs provide a way to characterize the asymptotic behavior of non-linear dynamical systems by measuring the mean exponential

* Corresponding author. Tel.: +213-740-0495; fax: +213-740-8071.
*E-mail address:* fudwadia@usc.edu (F.E. Udwadia).

[1] Computer code to compute LCEs is available at http:\\www.usc.edu\go\DynCon.

0096-3003/01/$ - see front matter 
PII: S0096-3003(99)00292-1

growth (or shrinking) of perturbations with respect to a nominal trajectory. LCEs are a measure of the sensitivity of the solutions of a given dynamical system to small changes in the initial conditions. One feature of chaos is the sensitive dependence on initial conditions; for a chaotic dynamical system at least one LCE must be positive. Since for non-chaotic systems all LCEs are non-positive, the presence of a positive LCE has often been used to establish if an attracting set is chaotic or not [2]. LCEs are used to study dynamical systems in almost every field, for example in celestial mechanics (see [3]), thermodynamics (see [4]), human physiology (see [5]), and in studies of meteorological phenomena like the 'El Niño' (see [6]).

In general, when computing the LCEs of a dynamical system, be it continuous or discrete, one usually performs a $QR$-factorization of the fundamental solution of the system (see [7–10]). The fundamental solution $Y$ is expressed as $Y = QR$, where $Q$ is an orthogonal matrix and $R$ is an upper triangular matrix. The LCEs are obtained from the diagonal elements of the upper triangular matrix $R$, which are functions of both the orthogonal matrix $Q$ and the Jacobian matrix of the system. The orthogonal matrix $Q$ is time dependent in the case of continuous systems and iteration dependent in the case of discrete systems. When dealing with computational methods, in either case, the orthogonality of $Q$ affects the accuracy of the LCEs. It has been recognized (see [9–12]) that it is very important to develop methods to compute the LCEs which preserve the orthogonality of $Q$. One way to preserve the orthogonality of $Q$ is by using Householder reflector matrices in order to obtain the QR-factorization. The efficient and numerically stable use of Householder reflector matrices in the computation of the LCEs was implemented by Von Bremen et al. [12] for discrete dynamical systems.

When dealing with discrete dynamical systems, the presence of errors in the orthogonality of $Q$ usually lead to inaccurate computational results. But such errors do not seem to prevent the various methods of computing LCEs from yielding *some* computational results (at least for all the systems encountered by us), although they may be inaccurate. On the other hand for continuous systems, errors in orthogonality can actually lead to a break down in the computation of LCEs due to overflows (or underflows) in the computations. We present an example of such break down when using the most prevalent method for computing LCEs.

In this paper, we present an approach to compute the LCEs for continuous dynamical systems that preserves the orthogonality of $Q$. Since the method preserves the orthogonality of $Q$, it is stable in the sense that it will not break down during computations. Also, since the method preserves orthogonality, the LCEs are obtained with greater numerical accuracy. Furthermore, the new method is more efficient than the method commonly prevalent in the literature. It requires the solution of fewer differential equations than normally needed with the usual method.

The general formulation for the computation of the LCEs using the *QR*-factorization is given in Section 2. Section 3 deals with what we call the *Q*-method (which is the method usually found in the literature). The new approach (the $e^S$-method) is presented in Section 4. In Section 5 we present the adaptation of the $e^S$-method to the special case of systems whose LCEs can be computed using a 2D system. Expressions to obtain the time evolution of the LCEs of general 2D systems are given in terms of a Ricatti equation and two quadratures. Closed form expressions for the time evolution of the LCEs for the special constant Jacobian case are also given. These closed form solutions of the time evolution of the LCEs are used in three examples; numerical results from the newly proposed method and the *Q*-method are compared with the exact values. Section 5 ends with a subsection on special systems that can be reduced to 2D systems for the purpose of computing LCEs. Numerical comparisons between the *Q*-method and the $e^S$-method are given for the forced Duffing's equation. In Section 6, we specialize the $e^S$-method to 3D systems. The Lorenz system is used to illustrate the accuracy of the $e^S$-method and also to illustrate the total break down of the *Q*-method in computing LCEs. The Appendix gives three results which are used in this paper, and are generally applicable to the computation of LCEs. Concluding remarks are given in Section 7.

## 2. Computation of the LCEs using the *QR*-factorization

Continuous dynamical systems are usually described by an ordinary differential equation of the form

$$\dot{y}(t) = f(y(t)), \quad y(0) = y_0, \tag{1}$$

where $y \in \mathbb{R}^n$, and $t \in \mathbb{R}$. The variational equation associated with the dynamical system described in (1) is given by

$$\dot{Y} = JY, \quad Y(y;0) = I, \tag{2}$$

where $Y \in \mathbb{R}^{n\times n}$. Here $I$ is the $n$ by $n$ identity matrix and $J$ is the $n$ by $n$ Jacobian matrix of $\dot{y} = f(y)$ at $(y;t)$. That the solution $Y$ depends on the trajectory of the dynamical system, is denoted by $Y(y;t)$. The $n$ Lyapunov exponents $\lambda_i$ are the logarithms of the eigenvalues $\mu_i$, $i = 1$ to $n$, of the matrix $\Lambda_y$ given by

$$\Lambda_y = \lim_{t\to\infty}\left[Y(y:t)^{\mathrm{T}}Y(y:t)\right]^{1/(2t)}. \tag{3}$$

To compute the LCEs one has to simultaneously solve the initial value problems given by (1) and (2). The solution to (1) is used to obtain the Jacobian at every point $(y;t)$ which is needed to solve (2). The direct solution of (2) presents numerical difficulties since the column vectors of $Y$ will computationally

converge toward the subspace with the largest expansion rate. To avoid this numerical difficulty the Lyapunov exponents for continuous dynamical systems are obtained by either performing a $QR$ or a singular value factorization of the variational equation. In this paper we focus on the $QR$ factorization method.

The basic idea behind the $QR$ factorization method is to obtain the decomposition of $Y$ into the product of an $n$ by $n$ orthogonal matrix $Q$ and an $n$ by $n$ upper triangular matrix $R$, that is $Y = QR$. Using the differential equations for $Q$, the Lyapunov characteristic exponents of the system can be then computed. The orthogonal matrix $Q$ can be expressed in two different forms. The method generally found in the literature does not utilize the special structure of $Q$. This method leads to $n^2$ differential equations to obtain $Q$. This paper proposes a new approach. We consider $Q$ as a rotation matrix and we express it as $Q = e^S$, where $S$ is a skew symmetric matrix. When this special structure of $Q$ is considered, we only need to obtain the differential equations for $S$, and from $S$, the matrix $Q$ can be constructed. The evolution of the skew symmetric matrix $S$ can be established through $n(n-1)/2$ differential equations. In this paper we call the first method the $Q$-method and the later approach the $e^S$-method.

## 3. The $Q$-method

What we refer to as the $Q$-method is the one generally found in the literature, for example see [9,11]. In this method $Q$ is obtained by solving a set of $n^2$ differential equations.

The $QR$ decomposition of $Y$ as $Y = QR$, together with the variational Eq. (2) gives

$$\dot{Q}R + Q\dot{R} = JQR, \quad Q(0)R(0) = I. \tag{4}$$

Premultiplication of (4) by $Q^{\mathrm{T}}$ and postmultiplication by $R^{-1}$ together with $Q^{\mathrm{T}}Q = I$ gives

$$Q^{\mathrm{T}}\dot{Q} + \dot{R}R^{-1} = Q^{\mathrm{T}}JQ, \quad Q(0) = I, \quad R(0) = I. \tag{5}$$

Observe that since $Q^{\mathrm{T}}Q = I$, the matrix $K = Q^{\mathrm{T}}\dot{Q}$ is a skew symmetric matrix and the product $\dot{R}R^{-1}$ is upper triangular since $R$ is upper triangular. These two observations and (5) give us the equation that defines $K$ as

$$K_{ij} = \begin{cases} (Q^{\mathrm{T}}JQ)_{ij}, & i > j, \\ 0, & i = j, \\ -(Q^{\mathrm{T}}JQ)_{ji}, & j > i. \end{cases} \tag{6}$$

From $K = Q^{\mathrm{T}}\dot{Q}$ we get

$$\dot{Q} = QK, \quad Q(0) = I. \tag{7}$$

Eq. (7) together with (6) yield the differential equation for $\dot{Q}$ in terms of $Q$ and $J$. Since $Q^{\mathrm{T}}\dot{Q}$ is skew symmetric, (4) yields the differential equations for $\rho_i = \ln(R_{ii})$, the logarithms of the diagonal elements of $R$, as

$$\dot{\rho}_i = \frac{\dot{R}_{ii}}{R_{ii}} = (Q^{\mathrm{T}}JQ)_{ii} \quad \text{with } \rho_i(0) = 0 \text{ for } i = 1, \ldots, n. \tag{8}$$

Denoting by $\lambda_i(t) = \ln(R_{ii})/t$ the time evolution of the LCEs, the LCEs are then given by

$$\lambda_i = \lim_{t\to\infty} \frac{\rho_i(t)}{t} = \lim_{t\to\infty} \lambda_i(t). \tag{9}$$

Note that the $n^2$ differential equations used in this formulation (and computation) for the elements of $Q$ are not independent. For the elements of $Q$ must be such that (1) the $l_2$ norm of each column is unity and (2) each column of $Q$ is orthogonal to every other column. Since this leads to $n + (n(n-1))/2$ relations which the $q_{ij}(t)$'s must satisfy, the number of independent $q_{ij}(t)$'s are $n(n-1)/2$.

## 4. The $e^S$-method

In general, the matrix $Q(t)$ obtained in the $QR$ decomposition $Y(t) = Q(t)R(t)$ is an orthogonal matrix, thus $\det(Q(t)) = \pm 1$. Since $Q(0) = I$ and the elements of $Q(t)$are continuous functions of time, if at some time $t > 0$, $\det(Q(t))$ becomes $-1$, then there is some time $\tau \in (0, t)$, such that $\det(Q(\tau)) = 0$. But this is impossible, since $Y(\tau)$ would then be singular. Thus for all $t$, $\det(Q(t)) = 1$. The 3 by 3 orthogonal matrices with $\det(Q) = +1$ are called rotation matrices, and the $n$ by $n$ orthogonal matrices (with a determinant equal to 1) form the $SOn$ group.

Any matrix belonging to the $SOn$ group can be expressed as the exponential of a skew symmetric matrix $S$ [13], i.e., $Q = e^S$. The main idea behind the $e^S$-method is to obtain the differential equations defining $S$. Solving these differential equations we obtain $S(t)$, and $Q(t)$ is then simply given by $Q(t) = e^{S(t)}$. The matrix $Q(t)$ by construction is then guaranteed to be orthogonal. The $n(n-1)/2$ lower diagonal elements of $S$ characterize all of $S$ and thus $Q$.

Thus compared to the $Q$-method, the $e^S$-method (1) guarantees that $Q(t)$ is orthogonal (which is not done by the $Q$-method), and (2) requires the solution of only $n(n-1)/2$ differential equations (instead of $n^2$ differential equations required by the $Q$-method) for obtaining $Q$.

To derive the differential equations for $S$ we start by replacing $Q$ with $e^S$ in (4) to get

$$\frac{\mathrm{d}e^S}{\mathrm{d}t}R + e^S\dot{R} = Je^S R, \quad S(0) = 0, \quad R(0) = I. \tag{10}$$

Using $Q^{\mathrm{T}} = e^{-S}$, Eq. (10) can be rewritten as

$$e^{-S}\frac{\mathrm{d}e^S}{\mathrm{d}t} + \dot{R}R^{-1} = e^{-S}Je^S. \tag{11}$$

In order to obtain the differential equations for $S$, we need to find $\mathrm{d}e^S/\mathrm{d}t$ and we can use the earlier observation that the product $e^{-S}(\mathrm{d}e^S/\mathrm{d}t)$ is skew symmetric and $\dot{R}R^{-1}$ is upper triangular. In general, the equations for $\dot{S}$ can be obtained by expanding the lower triangular part of $e^{-S}(\mathrm{d}e^S/\mathrm{d}t)$ and equating it to the lower triangular part of $e^{-S}Je^S$.

As in the $Q$-method, the logarithms of the diagonal elements of $R$ are given by considering only the diagonal elements of the matrix Eq. (11), that is,

$$\dot{\rho}_i = \frac{\dot{R}_{ii}}{R_{ii}} = \left(Q^{\mathrm{T}}JQ\right)_{ii} = \left(e^{-S}Je^S\right)_{ii} \quad \text{with } \rho_i(0) = 0 \text{ for } i = 1, \ldots, n. \tag{12}$$

As in Eq. (9), the LCEs are then given by

$$\lambda_i = \lim_{t\to\infty}\frac{\rho_i(t)}{t} = \lim_{t\to\infty}\lambda_i(t).$$

To illustrate the approach, we will specialize the equations to two and three dimensional systems. 2D systems are dealt with in Section 5, and 3D systems in Section 6.

## 5. Systems of dimension $n = 2$

In this section we specialize the expansion for the case $n = 2$. There are two reasons why we start with systems whose LCEs are obtained by using a 2D system of differential equations. First, as shown in the Appendix A and illustrated later on in this section, there are many chaotic systems whose Jacobians can be reduced to smaller 2D and 3D sub-systems for the purposes of computing their LCEs. Second, for the constant coefficient 2D LCE system one can obtain in closed form the exact time evolution of the LCEs. One can then compare these exact time evolutions with those computed using different methods, thereby testing their accuracy. We first establish all the differential equations needed to find the two LCEs of the system. Then we derive the closed form solutions for the special 2D case when the Jacobian is a constant matrix. Numerical examples are used to compare the accuracy of the $Q$ and the $e^S$-methods for the constant Jacobian matrix case.

Using functions of matrices and the eigenvalues of $S$, we can obtain an explicit form for $e^S$. Let

$$S = \begin{bmatrix} 0 & \theta \\ -\theta & 0 \end{bmatrix},$$

the eigenvalues of $S$ are $\mu_{1,2} = \pm\theta i$. Evaluating the function $f(x) = e^x$ over the spectrum of $S$ we get

$$e^S = \cos(\theta) I + \frac{\sin(\theta)}{\theta} S = \begin{bmatrix} \cos(\theta) & \sin(\theta) \\ -\sin(\theta) & \cos(\theta) \end{bmatrix} \tag{13}$$

which is as expected, since any planar rotation can be expressed as in Eq. (13). Differentiating (13) gives

$$\frac{de^S}{dt} = \begin{bmatrix} -\sin(\theta) & \cos(\theta) \\ -\cos(\theta) & -\sin(\theta) \end{bmatrix} \dot{\theta}. \tag{14}$$

Let the Jacobian of (1) be given by

$$J(t) = \begin{bmatrix} a(y;t) & m(y;t) \\ -k(y;t) & -c(y;t) \end{bmatrix}. \tag{15}$$

Then the right-hand side of (11) becomes

$$e^{-S} J e^S = \begin{bmatrix} -c\sin^2(\theta) + a\cos^2(\theta) - (m-k)\sin(\theta)\cos(\theta) & k\sin^2(\theta) + m\cos^2(\theta) + (a+c)\sin(\theta)\cos(\theta) \\ -m\sin^2(\theta) - k\cos^2(\theta) + (a+c)\sin(\theta)\cos(\theta) & a\sin^2(\theta) - c\cos^2(\theta) - (k-m)\sin(\theta)\cos(\theta) \end{bmatrix}. \tag{16}$$

Since the lower triangular element of $e^{-S}(de^S/dt)$ is just $-\dot{\theta}$, using the diagonal and lower triangular part in (11) we get the following system of differential equations:

$$\dot{\theta} = k\cos^2(\theta) + m\sin^2(\theta) - (a+c)\sin(\theta)\cos(\theta), \quad \theta(0) = 0, \tag{17}$$

$$\dot{\rho}_1 = a\cos^2(\theta) - c\sin^2(\theta) - (m-k)\sin(\theta)\cos(\theta), \quad \rho_1(0) = 0, \tag{18}$$

$$\dot{\rho}_2 = -c\cos^2(\theta) + a\sin^2(\theta) + (m-k)\sin(\theta)\cos(\theta), \quad \text{and} \quad \rho_2(0) = 0. \tag{19}$$

Using the transformation $x = \tan(\theta)$, Eq. (17) becomes the Riccati equation

$$x' = m(t)x^2 - \{a(t) + c(t)\}x + k(t), \quad x(0) = 0. \tag{20}$$

Using Eqs. (18) and (19) and integrating, we get the following system of equations:

$$\gamma_1(t) \equiv \rho_1(t) + \rho_2(t) = \int_0^t (a(\tau) - c(\tau))d\tau \tag{21}$$

and

$$\gamma_2(t) \equiv \rho_1(t) - \rho_2(t) = \int_0^t \{(a(\tau) + c(\tau))\cos(2\theta(\tau)) + (k(\tau) - m(\tau))\sin(2\theta(\tau))\}\mathrm{d}\tau. \quad (22)$$

From these equations, $\rho_1(t)$ and $\rho_2(t)$ can now be obtained as

$$\rho_1(t) = \frac{\gamma_1(t) + \gamma_2(t)}{2}, \quad (23)$$

and

$$\rho_2(t) = \frac{\gamma_1(t) - \gamma_2(t)}{2}. \quad (24)$$

Thus one obtains the LCEs by first solving the Ricatti equation (20), then evaluating the integrals in (21) and (22), and finally using (23) and (24) to compute $\rho_1(t)$ and $\rho_2(t)$. The time evolutions of the LCEs are then simply given by $\lambda_1(t) = \rho_1(t)/t$, and $\lambda_2(t) = \rho_2(t)/t$. By using the above steps one can compute the LCEs very accurately and efficiently, since the solution of the Ricatti equation can be obtained through accurate and efficient specialized methods (see [14]), and the integrals can be obtained by using quadrature methods which are also very accurate and efficient.

We note that from Eq. (21), the *sum of the time-evolving LCEs*, $\lambda_1(t) + \lambda_2(t)$, is simply the *time-average* of the Trace, $a(t) - c(t)$, of the Jacobian $J(t)$ of the 2D system (see Appendix A for a proof of this result for $n$-dimensional systems).

For the special case when the Jacobian is constant we can obtain the time evolution of $\theta$ as well as that of the Lyapunov exponents in an explicit form. The special case of a constant Jacobian is presented in the next section.

### *5.1. Closed form solution for the 2D case with constant Jacobian*

There are very few non-trivial systems for which we know the exact LCEs and even fewer for which we know the time evolution of the LCEs explicitly. It is well known that for a constant Jacobian the LCEs are given by the real parts of the eigenvalues of the Jacobian. However, the way the LCEs actually evolve in time has not been shown before in the literature even for the 2D case (as far as the authors know). In this section we present closed form expressions for the time evolution of the LCEs of the 2D case with a constant Jacobian. These closed from expressions allow us to compare the time evolution of the computed LCEs by a given method with the time evolution of the exact LCEs, and not just with the exact LCEs obtained in the limit. The closed form expressions of the time evolution of the LCEs also give some insight to their qualitative behavior, which depends on the parameter values of the Jacobian. The ex-

pressions for the time evolution of the LCEs take on three different forms depending on whether the discriminant of the right hand side of (20) is positive, zero or negative, leading to three qualitatively different equations for the LCEs.

We use the Jacobian as given in (15), but with the parameters $m$, $k$, $c$ and $a$, each a constant. We integrate Eq. (17), and then Eqs. (18) and (19) to obtain the time evolution of the LCEs in closed form.

The discriminant of the right-hand side of (20) is $(a+c)^2 - 4km$, and it will dictate the form of the solution of (20) and thus for (17), (18) and (19). Based on the discriminant we get the following three cases:

*Case* 1. The discriminant is zero. Completing the square on the right-hand side of (20), separating variables, and integrating, yields

$$\theta(t) = \tan^{-1}\left[\frac{(a+c)^2 t}{2m\{2+(a+c)t\}}\right]. \tag{25}$$

*Case* 2. The discriminant is negative. As with the previous case, after separation of variables, and integration, Eq. (20) becomes

$$x(t) = p\tan(mpt+z) + h, \tag{26}$$

where

$$h = \frac{a+c}{2m}, \quad p^2 = \frac{k}{m} - \left(\frac{a+c}{2m}\right)^2 \quad \text{and} \quad z = \arctan(-h/p). \tag{27}$$

In terms of the parameters of the Jacobian, $\theta(t)$ can thus be expressed as

$$\theta(t) = \arctan\left\{\frac{q}{2m}\tan\left[\frac{qt}{2} + \arctan\left(\frac{-a-c}{q}\right)\right] + \frac{a+c}{2m}\right\}$$
$$\text{with } q = \sqrt{4km-(a+c)^2}. \tag{28}$$

Expanding the tangent term in the last equation and simplifying we get

$$\theta(t) = \arctan\left\{\frac{2k\tan\left[\frac{\sqrt{4km-(a+c)^2}\,t}{2}\right]}{\sqrt{4km-(a+c)^2} + (a+c)\tan\left[\frac{\sqrt{4km-(a+c)^2}\,t}{2}\right]}\right\}. \tag{29}$$

*Case* 3. The discriminant is positive. Three sub-cases are considered.

*Case* 3i. The parameter $m = 0$. After integration, (20) becomes

$$\tan(\theta(t)) = x(t) = \frac{k - k\mathrm{e}^{-(a+c)t}}{a+c}. \tag{30}$$

*Case* 3ii. The product $mk < 0$. After separation of variables, (20) becomes

$$x(t) = p\tanh(z-mpt) + h, \tag{31}$$

where

$$h = \frac{a+c}{2m}, \quad p^2 = \left(\frac{a+c}{2m}\right)^2 - \frac{k}{m} \quad \text{and} \quad z = \operatorname{arctanh}(-h/p). \tag{32}$$

Again, in terms of the parameters of the Jacobian, $\theta(t)$ can thus be expressed as

$$\theta(t) = \arctan\left\{\frac{q}{2m}\tanh\left[\operatorname{arctanh}\left(\frac{-a-c}{q}\right) - \frac{qt}{2}\right] + \frac{a+c}{2m}\right\}$$
$$\text{with } q = \sqrt{(a+c)^2 - 4km}. \tag{33}$$

Expanding the hyperbolic tangent term in the last equation and simplifying we get

$$\theta(t) = \arctan\left\{\frac{2k}{\sqrt{(a+c)^2 - 4km}\coth\left[\frac{\sqrt{(a+c)^2-4km}t}{2}\right] + (a+c)}\right\}. \tag{34}$$

*Case* 3iii. The product $mk > 0$. After separation of variables, (20) becomes

$$x(t) = p\ \coth(z - mpt) + h, \tag{35}$$

where

$$h = \frac{a+c}{2m}, \quad p^2 = \left(\frac{a+c}{2m}\right)^2 - \frac{k}{m} \quad \text{and} \quad z = \operatorname{arccoth}(-h/p). \tag{36}$$

Again, in terms of the parameters of the Jacobian, $\theta(t)$ can thus be expressed as

$$\theta(t) = \arctan\left\{\frac{q}{2m}\coth\left[\operatorname{arccoth}\left(\frac{-a-c}{q}\right) - \frac{qt}{2}\right] + \frac{a+c}{2m}\right\}$$
$$\text{with } q = \sqrt{(a+c)^2 - 4km}. \tag{37}$$

Expanding the hyperbolic cotangent term in the last equation and simplifying we get

$$\theta(t) = \arctan\left\{\frac{2k}{\sqrt{(a+c)^2 - 4km}\coth\left[\frac{\sqrt{(a+c)^2-4km}t}{2}\right] + (a+c)}\right\}. \tag{38}$$

Now that expressions for $\theta(t)$ have been obtained, they can be used in the solution of Eqs. (18) and (19).

Eqs. (21) and (22) yield

$$\rho_1 + \rho_2 = (a-c)t \tag{39}$$

and

$$\rho_1 - \rho_2 = \int_0^t \{(a+c)\cos(2\theta) + (k-m)\sin(2\theta)\}\,\mathrm{d}\tau. \tag{40}$$

Using Eq. (17), Eq. (40) becomes,

$$\rho_1 - \rho_2 = \int_0^\theta \left\{ \frac{(a+c)\cos(2\theta) + (k-m)\sin(2\theta)}{k\cos^2(\theta) + m\sin^2(\theta) - (a+c)\sin(\theta)\cos(\theta)} \right\} \mathrm{d}\theta. \tag{41}$$

Setting $u = k\cos^2(\theta) + m\sin^2(\theta) - (a+c)\sin(\theta)\cos(\theta)$, we obtain

$$\rho_1 - \rho_2 = \int_k^u \frac{-\mathrm{d}\zeta}{\zeta} = -\ln(u/k). \tag{42}$$

From Eqs. (39) and (42),

$$\rho_1 = \frac{(a-c)t}{2} - \frac{\ln(u/k)}{2} \tag{43}$$

and

$$\rho_2 = \frac{(a-c)t}{2} + \frac{\ln(u/k)}{2}. \tag{44}$$

The time evolution of the Lyapunov exponents ($\lambda_1(t)$ and $\lambda_2(t)$) can now be obtained by using (43) and (44) as

$$\lambda_1(t) = \frac{(a-c)}{2} - \frac{\ln(u/k)}{2t} \tag{45}$$

and

$$\lambda_2(t) = \frac{(a-c)}{2} + \frac{\ln(u/k)}{2t}. \tag{46}$$

Recall that

$$\lambda_i = \lim_{t\to\infty} \frac{\rho_i(t)}{t},$$

and by (45) and (46) we have

$$\lambda_i = \lim_{t\to\infty} \lambda_i(t), \quad i = 1, 2.$$

The time evolution of the LCEs can be obtained by replacing the appropriate form for $\theta(t)$ (according to the discriminant) into (45) and (46). When replacing the appropriate expression for $\theta(t)$, cancellations will occur. If no precautions are taken with regard to these cancellations, then computational problems may develop when evaluating (45) and (46) for large $t$. After taking into account cancellations, the expressions for $u(t)$ and $\lambda_i(t)$ for the three cases take the following forms:

*Case* 1. When the discriminant equals zero

$$u(t) = \frac{4k\cos^2(\theta)}{(2+(a+c)t)^2}, \tag{47}$$

and the time evolution of the LCEs is given by

$$\lambda_{1,2}(t) = \frac{a-c}{2} \pm \frac{\ln[(km+k^2)t^2+(a+c)t+1]}{2t}. \tag{48}$$

In the special case when $k = 0$, Eq. (48) still holds and the time evolution of the LCEs are simply given by [2] $\lambda_1(t) = a$, and $\lambda_2(t) = -c$ (observe that when $k = 0$, then $a = -c$).

*Case* 2. When the discriminant is negative, with $p$, $h$ and $z$, as in (27)

$$u(t) = mp^2\cos^2(\theta)\sec^2(mpt+z), \tag{49}$$

and the time evolution of the LCEs is given by

$$\lambda_{1,2}(t) = \frac{a-c}{2} \mp \frac{\ln[2m^2p^2/k]}{2t} \pm \frac{\ln[k+m+(m-k+2mh^2)\cos 2(mpt+z)+(a+c)p\sin 2(mpt+z)]}{2t}. \tag{50}$$

Note that for the negative discriminant case we must always have that $km > 0$.

*Case* 3. When the discriminant is positive, we have the following sub-cases:

*Case* 3i. When the parameter $m = 0$, then

$$u(t) = \frac{k(a+c)^2 e^{-(a+c)t}}{(a+c)^2 + k(1-e^{-(a+c)t})^2}, \tag{51}$$

and the time evolution of the LCEs is given by

$$\lambda_{1,2}(t) = \frac{a-c}{2} \mp \frac{\ln\left\{(a+c)^2 e^{-(a+c)t}/((a+c)^2+k(1-e^{-(a+c)t})^2)\right\}}{2t}. \tag{52}$$

*Case* 3ii. When the product $mk < 0$, with $p$, $h$ and $z$ as in (32)

$$u(t) = -mp^2\cos^2(\theta)\sec h(z-mpt), \tag{53}$$

[2] For this special upper triangular Jacobian the LCEs are directly given by Corollary 2 in Appendix A.

and the time evolution of the LCEs is given by

$$\lambda_{1,2}(t) = \frac{a-c}{2} \mp \frac{\ln[4mp^2/k]}{2t} \pm \frac{\ln[2(k/m+1) + \{(p-h)^2+1\}e^{-2(z-mpt)} + \{(p+h)^2+1\}e^{2(z-mpt)}]}{2t}. \tag{54}$$

*Case* 3iii. When the product $mk > 0$, with $p$, $h$ and $z$ as in (36)

$$u(t) = mp^2 \cos^2(\theta)\mathrm{cosech}^2(z - mpt), \tag{55}$$

and the time evolution of the LCEs is given by

$$\lambda_{1,2}(t) = \frac{a-c}{2} \mp \frac{\ln[-4mp^2/k]}{2t} \pm \frac{\ln[-2(k/m+1) + \{(p-h)^2+1\}e^{-2(z-mpt)} + \{(p+h)^2+1\}e^{2(z-mpt)}]}{2t}. \tag{56}$$

In the special Case 3i when $k = 0$, as before, the time evolution of the LCEs are simply given by $\lambda_1(t) = a$, and $\lambda_2(t) = -c$.

Depending on the parameter values in the Jacobian matrix, the *time evolution* of the LCEs for a constant Jacobian matrix are thus obtained in *closed form* from Eqs. (48), (50), (52), (54) and (56).

For a constant Jacobian $J$, the LCEs are the real parts of the eigenvalues of $J$. In the 2D case, the eigenvalues of $J$ are given by

$$\mu = \frac{a - c \pm \sqrt{(c-a)^2 - 4(km - ac)}}{2}. \tag{57}$$

Thus the LCEs for the case

(1) when the discriminant is non-positive, are given by

$$\lambda_{1,2} = \frac{a-c}{2}; \tag{58}$$

(2) when the discriminant is positive, are given by

$$\lambda_{1,2} = \frac{a - c \pm \sqrt{(c-a)^2 - 4(km - ac)}}{2}. \tag{59}$$

On taking the limit as $t$ goes to infinity in Eqs. (48), (50), (52), (54) and (56) convergence to the exact LCEs given in (58), and (59) occurs, as expected.

In the next section we present numerical comparisons of the evolution of the LCEs computed using the $Q$-method and the $e^S$-method, with those obtained from the exact, closed form solutions derived in this section.

### 5.2. Numerical examples for the 2D constant Jacobian case

The three examples shown in this section correspond to the linear single-degree-of-freedom oscillator described by the equation

$$\ddot{y} + c\dot{y} + ky = 0 \tag{60}$$

with appropriate initial conditions.

Using the transformation $y_1(t) = y(t)$ and $y_2(t) = \dot{y}(t)$, the system simply becomes the first order system

$$\begin{bmatrix} \dot{y}_1 \\ \dot{y}_2 \end{bmatrix} = \begin{bmatrix} y_2 \\ -cy_2 - ky_1 \end{bmatrix}, \quad \text{with the Jacobian} \quad J = \begin{bmatrix} 0 & 1 \\ -k & -c \end{bmatrix}.$$

Comparing $J$ with the expression of the Jacobian in (15), here $a = 0$ and $m = 1$.

The case of critical damping in Eq. (60) corresponds to the zero discriminant case of the right-hand side (20). This case will be shown first for the parameter values of $a = 0,\ m = 1,\ c = 2$, and $k = 1$. The underdamped case in Eq. (60) corresponds to the negative discriminant case of the right-hand side of (20), and it will be illustrated here with the parameter values of $a = 0,\ m = 1,\ c = 1$, and $k = 1$. We will also show an example of an overdamped case in Eq. (60) (the overdamped case with $mk > 0$ corresponds to a positive discriminant of the right-hand side of (20)), using the parameter values of $a = 0,\ m = 1,\ c = 3$, and $k = 1$.

The LCEs for the three cases of the discriminant are computed using the $e^S$ and the $Q$-method. Both methods were computationally implemented using a fourth order Runge–Kutta integrator with a fixed time step size of 0.1, and in each case the inital conditions were $y_1(0) = 1$ and $y_2(0) = 0$. All computations were performed using Matlab with a machine precision of $2.2 \times 10^{-16}$. For the $Q$-method system (1) together with the systems given in (7) and (8) were solved. For the $e^S$-method, system (1) and Eqs. (17)–(19) were solved. Comparisons with the exact, closed form, results given by Eqs. (48), (50) and (56) we performed.

As will be seen next, the $e^S$-method gives more accurate results than the $Q$-method for the examples presented. The errors in computing the time evolution of the LCEs can be defined as the difference between the exact and the computed values for the $Q$-method and the $e^S$-method. As an additional measure of the numerical accuracy of the methods, the error in orthogonality $\|Q^{\mathrm{T}}Q - I\|_2$ is given for the two methods.

The first case deals with a discriminant equal to zero ($a = 0,\ m = 1,\ c = 2$ and $k = 1$). The time evolution of the two LCEs is given in Fig. 1 (the values reported come from Eq. (48)). From Fig. 1 we can observe that the LCEs seem to be asymptotically approaching the expected values $\lambda_{1,2} = -1$ (for this case the exact LCEs are $\lambda_{1,2} = -1$, as given by Eq. (58)).

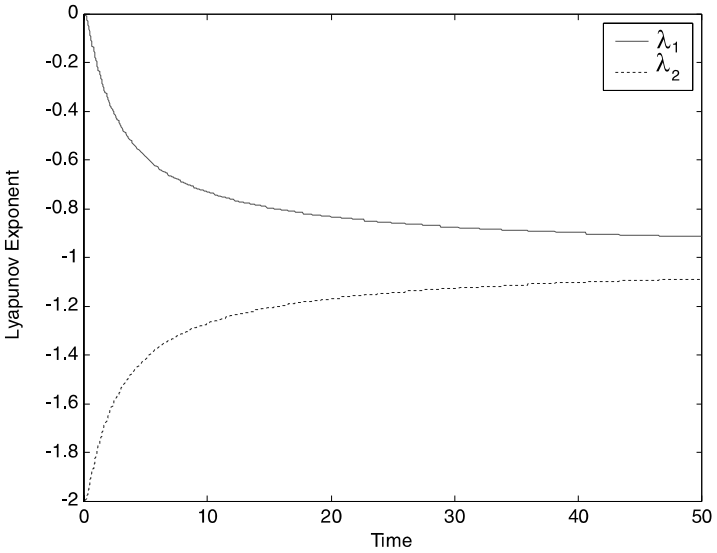


Fig. 1. Time evolution of the LCEs for the zero discriminant case with $a = 0,\ m = 1,\ c = 2$ and $k = 1$, using closed form solutions.

Fig. 2(a) and (b) show the error in the time evolution of the LCEs for the $Q$- and the $e^S$-methods for the first and the second LCE, respectively. From the figures, for the $e^S$-method, the error in the LCEs reduces (approaches zero) as time increases. On the other hand, for the $Q$-method the errors in the LCEs seem to be approaching nonzero values asymptotically.

Fig. 3 presents the error in orthogonality for both methods as a function of time. The error in orthogonality for the $e^S$-method is within the machine precision (i.e., $\approx 2.2 \times 10^{-16}$), while for the $Q$-method the error approaches $5 \times 10^{-6}$.

We next present an example with a negative discriminant ($a = 0,\ m = 1,\ c = 1$ and $k = 1$). Fig. 4 shows the time evolution of the LCEs of the system when using the exact equation (Eq. (50)). Both LCEs are asymptotically approaching the exact values of $\lambda_1 = \lambda_2 = -1/2$, as given by Eq. (58) in an oscillatory manner.

Fig. 5(a) and (b) show the error in the time evolution of the LCEs for the $Q$- and the $e^S$-methods for the first and the second LCEs, respectively. In both cases the error is smaller for the $e^S$-method. As time increases the error for the $Q$-method oscillates with increasing amplitude, while the error in the $e^S$-method oscillates with slightly decreasing amplitude. The errors in the time evolution of the LCEs for the $Q$-method though being oscillatory in nature are always positive, while the corresponding errors for the $e^S$-method oscillate about zero.

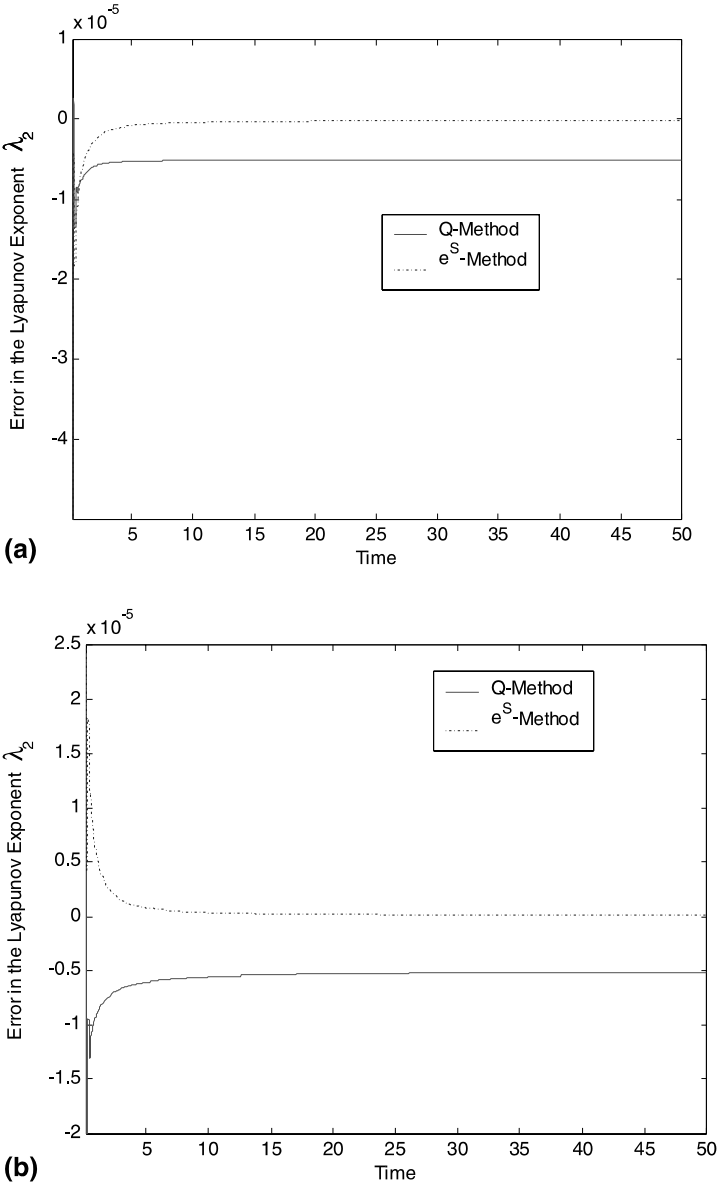


Fig. 2. (a) Error in the time evolution of the LCE $\lambda_1$ for the $Q$- and $e^S$-methods. Values for the zero discriminant case with $a = 0,\ m = 1,\ c = 2$, and $k = 1$. (b) Error in the time evolution of the LCE $\lambda_2$ for the $Q$- and $e^S$-methods. Values for the zero discriminant case with $a = 0,\ m = 1,\ c = 2$ and $k = 1$.

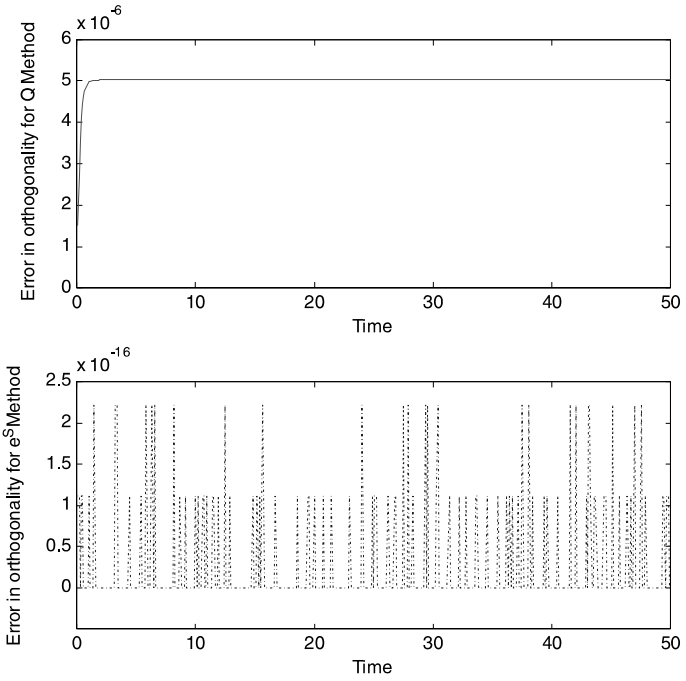


Fig. 3. Error in orthogonality for the $Q$- and the $e^S$-methods as a function of time. Values for the zero discriminant case with $a = 0,\ m = 1,\ c = 2$ and $k = 1$.

Fig. 6 presents the error in orthogonality for both methods as a function of time. The error in orthogonality for the $e^S$-method remains within the machine precision, while for the $Q$-method the error increases as time increases. When larger values of time are considered the same trend of an increasing error in orthogonality in the $Q$-method can be observed.

The last case shows an example of a positive discriminant ($a = 0, m = 1,\ c = 1$ and $k = 1$). Fig. 7 shows the time evolution of the LCEs of the system when using the exact equation (Eq. (56)). Both LCEs are asymptotically approaching the exact values (as in Eq. (59)) of $\lambda_1 = -0.382$ and $\lambda_2 = -2.618$.

Fig. 8(a) and (b) show the error in the time evolution of the LCEs for the $Q$-method and the $e^S$-method for the first and the second LCEs, respectively. For both LCEs the error for the $e^S$-method reduces as time increases, and the error approaches zero. On the other hand, the errors in the LCEs for the $Q$-method seem to approach nonzero values.

Fig. 9 presents the error in orthogonality for both methods as a function of time. The error in orthogonality for the $e^S$-method is within the machine precision, while for the $Q$-method it approaches a value close to $1.7 \times 10^{-5}$.

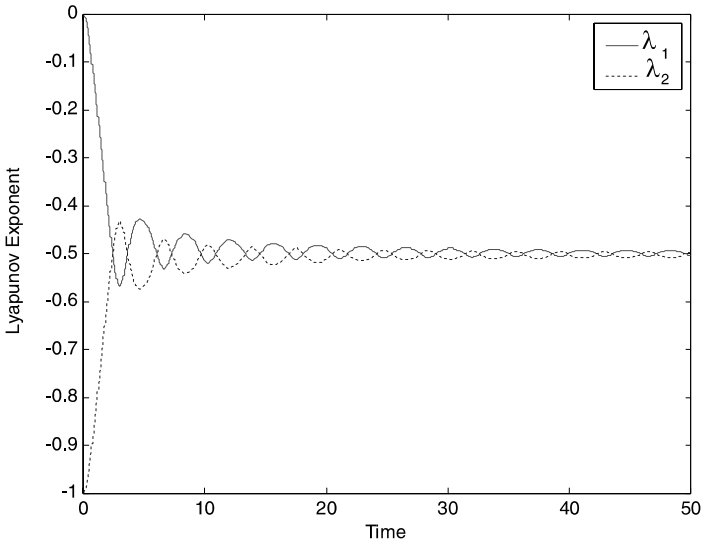


Fig. 4. Time evolution of the LCEs for the negative discriminant case with $a = 0,\ m = 1,\ c = 1$ and $k = 1$, using closed form solutions.

All three cases shown reflect that for the $e^S$-method as time increases, the error in the time evolution of the LCEs approaches zero. Thus the LCEs computed through the $e^S$-method seem to converge towards the exact value. In the case of the $Q$-method, all three examples show that the errors in the time evolution of the LCEs do not approach zero. For the zero and positive discriminant cases, the errors in the LCEs seem to approach finite nonzero values, and for the negative discriminant case, the errors are oscillatory with increasing amplitudes (for the parameter values shown). This implies that the LCEs computed through the $Q$-method could be quite different from the exact ones.

The superiority of the $e^S$-method over the $Q$-method is also reflected by the fact that the $Q$-method has always a significantly larger error in orthogonality than the $e^S$-method. We specifically draw attention to the case with the negative discriminant, in which the error in orthogonality for the $Q$-method shows an increasing trend with time.

### 5.3. Special 2D systems

Often, higher order systems ($n > 2$) can be decomposed into smaller ones for the purposes of computing their LCEs, as is shown in Appendix A. Even

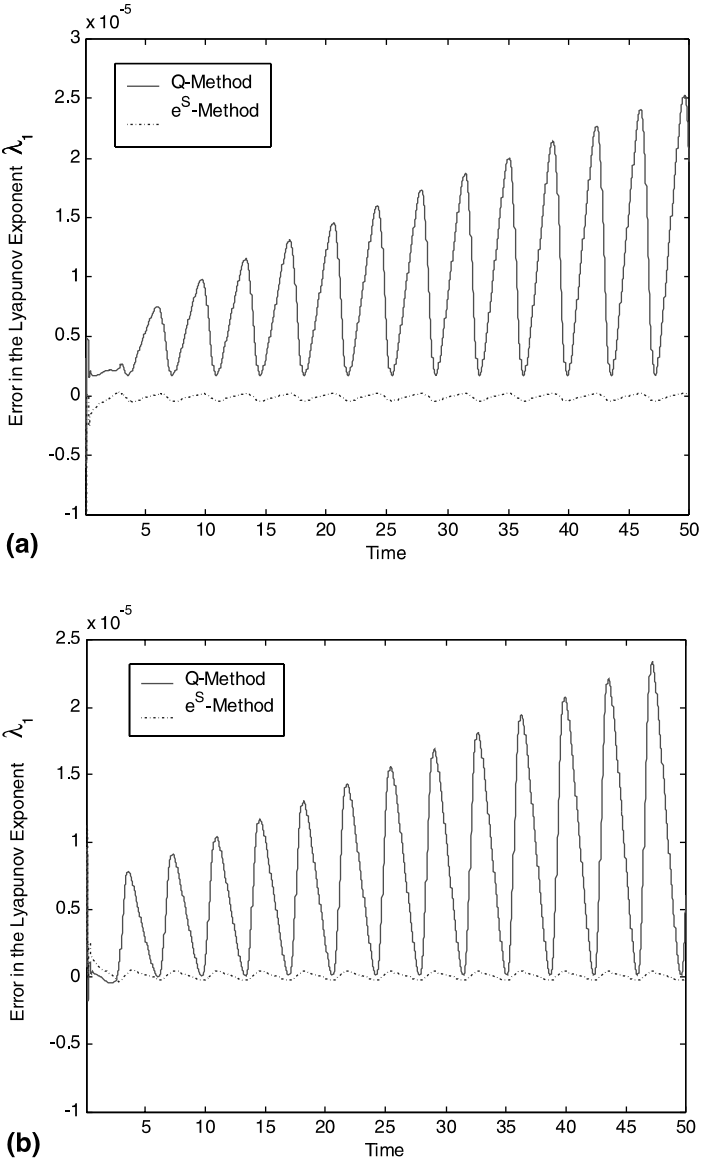


Fig. 5. (a) Error in the time evolution of the LCE $\lambda_1$ for the $Q$- and $e^S$-methods. Values for the negative discriminant case with $a = 0,\ m = 1,\ c = 1$ and $k = 1$. (b) Error in the time evolution of the LCE $\lambda_2$ for the $Q$- and $e^S$-methods. Values for the negative discriminant case with $a = 0,\ m = 1,\ c = 1$ and $k = 1$.

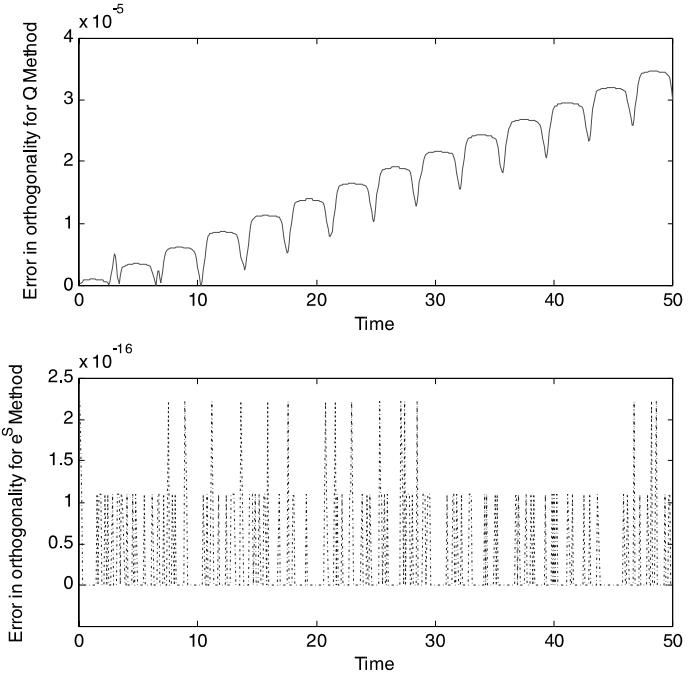


Fig. 6. Error in orthogonality for the $Q$- and the $e^S$-methods as a function of time. Values for the negative discriminant case with $a = 0,\ m = 1,\ c = 1$ and $k = 1$.

though continuous autonomous 2D systems cannot exhibit chaotic behavior, the equations developed in the previous subsection can be used to establish the non-trivial LCEs for special, higher-dimensional, systems which could exhibit chaotic behavior (see [9]). Many times, for LCE computations, they can be reduced to 2D sub-systems.

As an example, consider a forced oscillator whose response, is described by an equation of the form

$$\ddot{y} + g(y, \dot{y}, t) = h(t), \quad y(0) = y_0 \quad \text{and} \quad \dot{y}(0) = v_0. \tag{61}$$

Often, periodic forcing of such a system, with $h(t) = h(t + T)$, can cause the response to be chaotic. Using the substitutions $y_1 = y$, $y_2 = \dot{y}$ and $y_3 = t$, we can rewrite the non-autonomous system (61) as the 3D autonomous system

$$\begin{bmatrix} \dot{y}_1 \\ \dot{y}_2 \\ \dot{y}_3 \end{bmatrix} = \begin{bmatrix} y_2 \\ h(y_3) - g(y_1, y_2, y_3) \\ 1 \end{bmatrix} \quad \text{and} \quad \begin{bmatrix} y_1(0) \\ y_2(0) \\ y_3(0) \end{bmatrix} = \begin{bmatrix} y_0 \\ v_0 \\ 0 \end{bmatrix}. \tag{62}$$

The Jacobian of the 3D autonomous system given in (62) is singular and the elements in its third row are all zero. Because of Eq. (2), this implies that $Y_{31}(t)$,

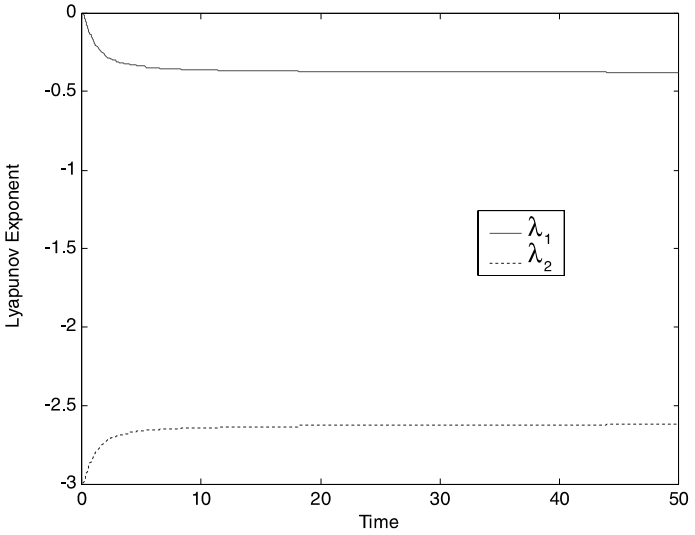


Fig. 7. Time evolution of the LCEs for the positive discriminant case with $a = 0,\ m = 1,\ c = 1$ and $k = 1$, using closed form solutions.

$Y_{32}(t)$ and $Y_{33}(t)$ are each constants. Using the initial condition $Y(0) = I$, we then have that $Y_{31} = 0$, $Y_{32} = 0$ and $Y_{33} = 1$. Since $Y$ is non-singular, then $Y$ has the $QR$-factorization $Y = QR$, and $Y$ can therefore be written as

$$\begin{bmatrix} Y_{11} & Y_{12} & Y_{13} \\ Y_{21} & Y_{22} & Y_{23} \\ 0 & 0 & 1 \end{bmatrix} = \begin{bmatrix} Q_{11} & Q_{12} & 0 \\ Q_{21} & Q_{22} & 0 \\ 0 & 0 & 1 \end{bmatrix} \begin{bmatrix} R_{11} & R_{12} & R_{13} \\ 0 & R_{22} & R_{23} \\ 0 & 0 & R_{33} \end{bmatrix}. \tag{63}$$

In order to find the LCEs of (61) we only need to determine the time evolution of $R_{11}$ and $R_{22}$, since $R_{33} \equiv 1$. Thus for the purpose of computing the LCEs we only need to consider the 2D subsystem of the form (see Appendix A for more general results)

$$\dot{\tilde{Y}} = \tilde{J}\tilde{Y}, \quad \tilde{Y}(0) = I, \tag{64}$$

where, for convenience, we explicitly write out the first equation (64) as

$$\dot{\tilde{Y}} = \begin{bmatrix} \dot{\tilde{Y}}_{11} & \dot{\tilde{Y}}_{12} \\ \dot{\tilde{Y}}_{21} & \dot{\tilde{Y}}_{22} \end{bmatrix} = \begin{bmatrix} 0 & 1 \\ -\frac{\partial g(y_1,y_2,y_3)}{\partial y_1} & -\frac{\partial g(y_1,y_2,y_3)}{\partial y_2} \end{bmatrix} \begin{bmatrix} \tilde{Y}_{11} & \tilde{Y}_{12} \\ \tilde{Y}_{21} & \tilde{Y}_{22} \end{bmatrix}. \tag{65}$$

The variational equations (64) and (65) given above correspond to the variational equations of a 2D system. Since $R_{33} = 1$, one LCE of the 3D system (62) is always zero.

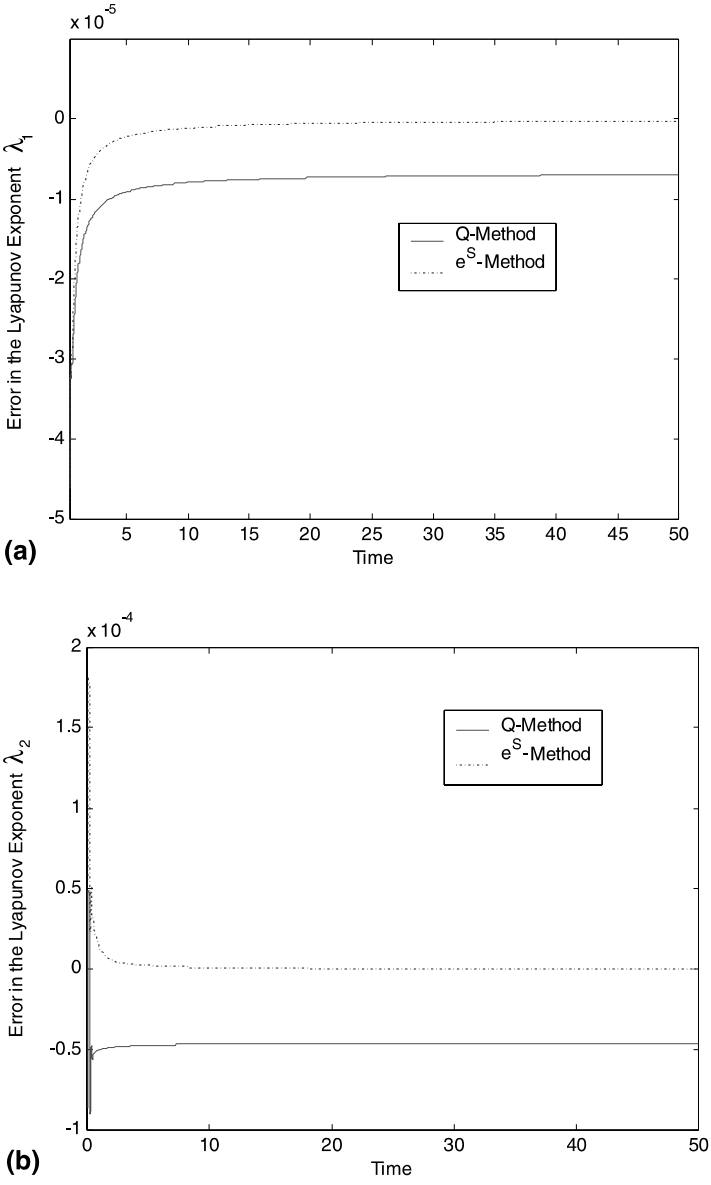


Fig. 8. (a) Error in the time evolution of the LCE $\lambda_1$ for the $Q$- and e$^S$-methods. Values for the positive discriminant case with $a = 0,\ m = 1,\ c = 1$ and $k = 1$. (b) Error in the time evolution of the LCE $\lambda_2$ for the $Q$- and e$^S$-methods. Values for the positive discriminant case with $a = 0,\ m = 1,\ c = 1$ and $k = 1$.

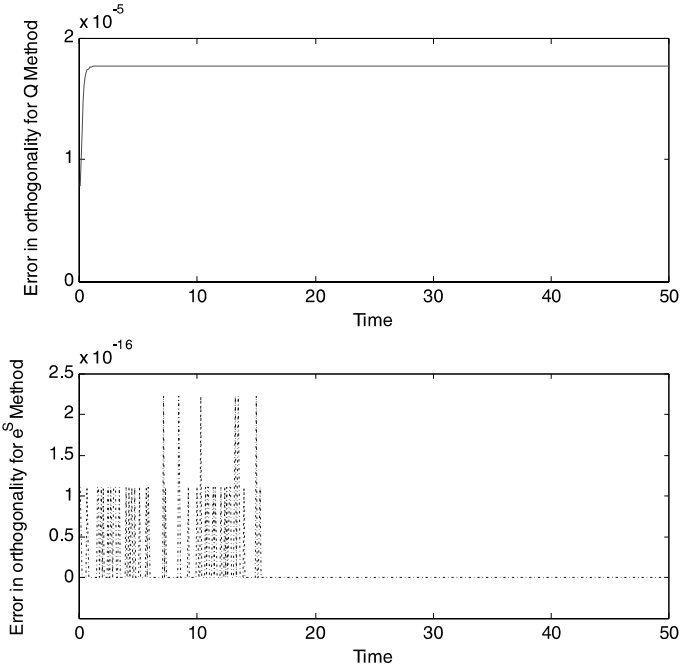


Fig. 9. Error in orthogonality for the $Q$- and the e$^S$-methods as a function of time. Values for the positive discriminant case with $a = 0,\ m = 1,\ c = 1$ and $k = 1$.

More generally, suppose the Jacobian of (2) has the following special upper-triangular block structure [3]:

$$J = \begin{bmatrix} J_1 & J_2 \\ O & J_3 \end{bmatrix}, \tag{66}$$

where the matrix block $J_1$ is $m$ by $m$, block $J_2$ is $m$ by $p$, block $J_3$ is a $p$ by $p$ upper triangular matrix, and $O$ is a $p$ by $m$ zero matrix, with $m + p = n$. (For the Jacobian corresponding to Eq. (62), we have $m = 2, p = 1$.) Then the solution $Y$ of the initial value problem (2) has the same structure as $J$ and it has a $QR$-decomposition as given below.

$$Y = \begin{bmatrix} Y_1 & Y_2 \\ O & Y_3 \end{bmatrix} = \begin{bmatrix} Q_1 & \tilde{O} \\ O & I_p \end{bmatrix} \begin{bmatrix} R_1 & R_2 \\ O & R_3 \end{bmatrix}, \tag{67}$$

where $Y_1$, $R_1$ and $Q_1$ are $m$ by $m$, with $R_1$ upper triangular, and $Q_1$ orthogonal, $Y_2$, $R_2$ and $\tilde{O}$ are $m$ by $p$, where $\tilde{O}$ is a zero matrix, $Y_3$, $R_3$ and $I_p$ are $p$ by $p$, with

[3] A matrix is called block upper triangular if it has square matrices along the diagonal with zeros in all entries below its block diagonal structure and where the elements above the diagonal blocks need not be zero.

$R_3$ upper triangular and $I_p$ an identity matrix, and $O$ is a $p$ by $m$ zero matrix. A proof of the result is shown in Appendix A (Result 1 and Corollary 1).

The above result can be used to reduce the system of equations necessary to find the LCEs of a system that has a Jacobian with a structure as given in (66). In order to determine $m$ of the LCEs, one just has to consider the subsystem

$$\dot{Y}_1 = J_1 Y_1, \quad Y_1(0) = I_m. \tag{68}$$

The remaining $p$ LCEs can be obtained by simple quadrature as

$$\lambda_i(t) = \frac{1}{t}\int_0^t (J_3(\tau))_{ii}\,\mathrm{d}\tau \quad \text{for } i = m+1,\ldots,n. \tag{69}$$

A proof of the last result is shown in the Appendix A (Result 2, and Corollary 2).

In the above case (Eq. (66)) the structure of the Jacobian was utilized to reduce the order of the system for purposes of finding the LCEs. In general, when the Jacobian matrix has a block-upper-triangular structure[2] with many blocks along the diagonal, its structure can similarly be used to reduce the system to several smaller subsystems when determining the LCEs. Detailed results related to this general case may be found in the Appendix A. Such reductions to smaller subsystems can lead to substantial savings in computational costs, and often, improved computational accuracy of the LCEs. As an example, consider the forced Duffing equation

$$\ddot{y} + C\dot{y} + y^3 = B\cos(t) \quad \text{with } y(0) = y_0 \text{ and } \dot{y}(0) = v_0, \tag{70}$$

which describes a periodically driven oscillator. It is of the form (61) with $g(y,\dot{y}) = C\dot{y} + y^3$ and $h(t) = B\cos(t)$ and can be rewritten in the form (62). From our previous discussion, one LCE of (70) is zero and the other two can be computed by considering the reduced system given by (64) and (65). The Jacobian $\tilde{J}$ for the reduced system corresponding to (70) is then

$$\tilde{J} = \begin{bmatrix} 0 & 1 \\ -\frac{\partial g(y_1,y_2)}{\partial y_1} & -\frac{\partial g(y_1,y_2)}{\partial y_2} \end{bmatrix} = \begin{bmatrix} 0 & 1 \\ -3y_2^2 & -C \end{bmatrix}. \tag{71}$$

Using Eq. (21) for this Jacobian we get $\rho_1 + \rho_2 = -Ct$. Therefore, the time-evolving nontrivial LCEs of the Duffing equation must satisfy the following relation:

$$\lambda_1(t) + \lambda_2(t) = -C. \tag{72}$$

Since the sum of the time-evolving LCEs [4] is constant, this sum can be used as an easy-to-compute indicator of the accuracy of the different methods used for

[4] See Appendix A (Result 3), where it is shown that the sum of the time evolving LCEs is equal to the time average of the trace of the Jacobian.

Table 1
Comparison of computed LCEs for Duffing's equation

| B | Moon [15] | Ueda [16] | $Q$-method | | | $e^S$-method | | |
|---|---|---|---|---|---|---|---|---|
| | $\lambda_1$ | $\lambda_1$ | $\lambda_1$ | $\lambda_2$ | Error in Sum | $\lambda_1$ | $\lambda_2$ | Error in Sum $\times 10^{-12}$ |
| 9.9 | 0.012 | 0.065 | 0.0044 | −0.1031 | 0.0013 | 0.0192 | −0.1192 | 0.3346 |
| 10 | 0.094 | 0.102 | 0.0651 | −0.1638 | 0.0013 | 0.0914 | −0.1914 | 0.3389 |
| 11 | 0.114 | 0.114 | 0.1099 | −0.2085 | 0.0014 | 0.1134 | −0.2134 | 0.3352 |
| 12 | 0.143 | 0.149 | 0.1349 | −0.2330 | 0.0019 | 0.1405 | −0.2405 | 0.3362 |
| 13 | 0.167 | 0.182 | 0.1487 | −0.2465 | 0.0022 | 0.1644 | −0.2644 | 0.3328 |
| 13.3 | 0.174 | 0.183 | 0.1501 | −0.2480 | 0.0021 | 0.1604 | −0.2604 | 0.3400 |

computing the LCEs (see Appendix A). Using the relation in Eq. (72), one can obtain an estimate of the numerical accuracy of computed LCEs.

Table 1 shows the computed LCEs for Duffing's equation given by different authors (and methods) for different $B$ values and a fixed value of $C = 0.1$. The table is an extension of that given in [15], where we have included our results using the $Q$- and the $e^S$-methods, for comparison. A fourth order Runge–Kutta scheme with a fixed step-size of 0.01 was used to compute the LCEs for the $Q$- and the $e^S$-methods. The initial conditions of the Duffing equation used to compute the LCEs by the $Q$- and the $e^S$-methods were $y_1(0) = 0$ and $y_2(0) = -6$. The column labeled 'Error in Sum' corresponds to the error in the sum of the LCEs (i.e., $\lambda_1 + \lambda_2 + 0.1$).

Among the computed LCEs by the different methods shown in the table, the closest agreement occurs between the values from the $e^S$-method and the values from Moon [15] (here reported for a final value of $t = 800\pi$). When comparing the results from the $Q$- and the $e^S$-methods, we note that the ratio of the error in the sum of the LCEs for the $Q$-method to that for the $e^S$-method is of order of $10^{10}$.

The following numerical results correspond to the computation of the LCEs using the $Q$- and the $e^S$-methods with the parameters of $B = 9.9$ and $C = 0.1$, and the initial conditions given before.

Fig. 10 shows the time evolution of the nontrivial LCEs for the Duffing equation when using the $Q$- and the $e^S$-methods (the first 50 s are not plotted in order to be able to see the asymptotic behavior). The LCEs at time $t = 2,513.3 \approx 800\pi$ are $\lambda_1 = 0.0192$ and $\lambda_2 = -0.1192$ for the $e^S$-method, and $\lambda_1 = 0.0044$ and $\lambda_2 = -0.1031$ for the $Q$-method.

Fig. 11 shows $\lambda_1 + \lambda_2 + 0.1$ as a function of time for the $Q$- and the $e^S$-methods. The large difference in the errors of the sum of the LCEs between the two methods can be observed on the plot, the error for the $Q$-method is in the order of $10^{-3}$, while for the $e^S$-method the error is practically zero at the scale of the plot.

Fig. 12 shows that the error in the sum of the LCEs for the $e^S$-method is of the order of $10^{-13}$.

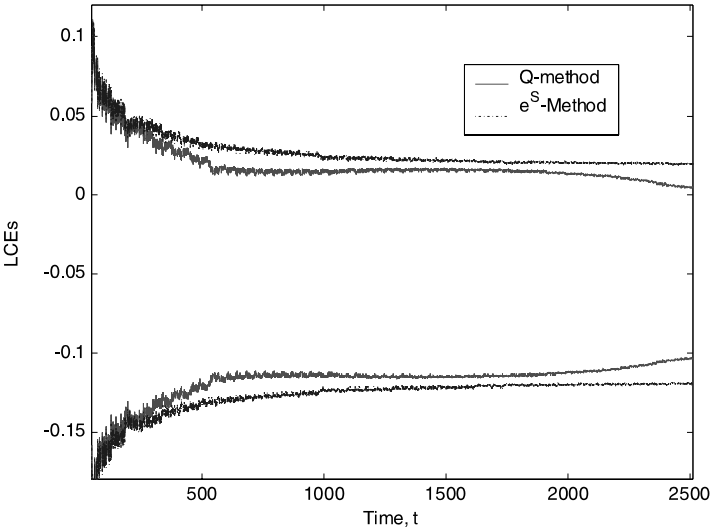


Fig. 10. Computed LCEs versus time for the Duffing equation using the $Q$- and the $e^S$-method.

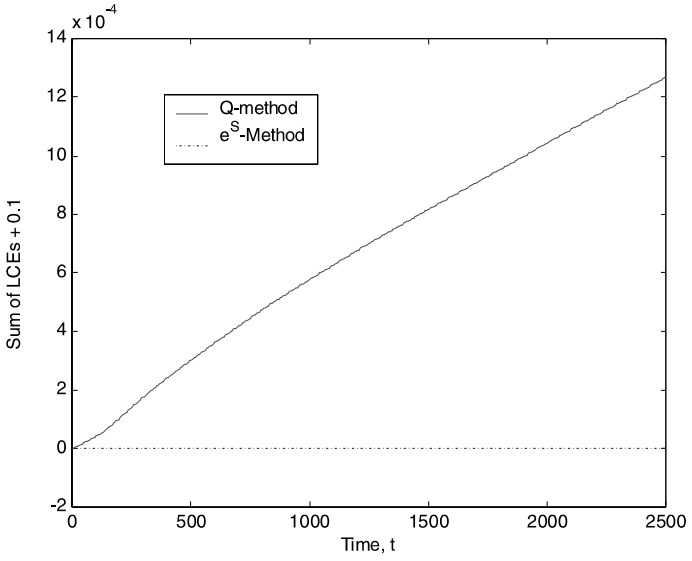


Fig. 11. Error in the sum of the LCEs ($\lambda_1 + \lambda_2 + 0.1$) as a function of time for the Duffing equation using the $Q$- and the $e^S$-method.

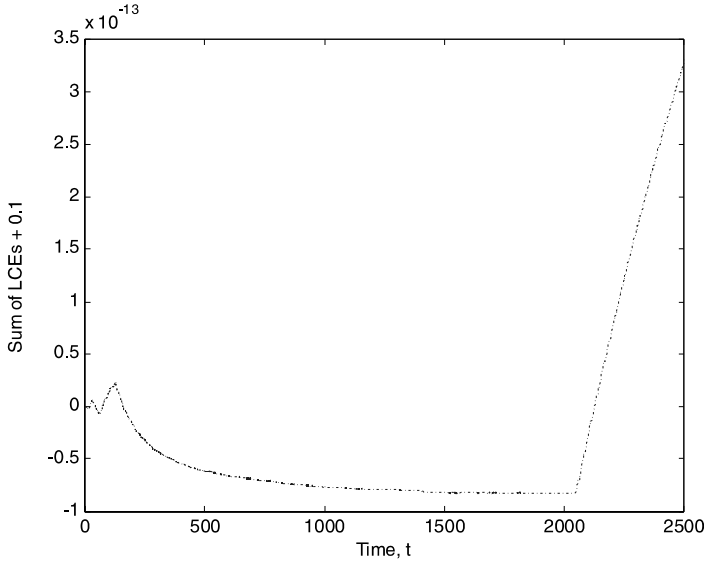


Fig. 12. Error in the sum of the LCEs ($\lambda_1 + \lambda_2 + 0.1$) as a function of time for the Duffing equation using the $e^S$-method.

Fig. 13 shows the error in orthogonality $\|Q^{\mathrm{T}}Q - I\|_2$ for the $Q$- and the $e^S$-methods. The figure clearly shows that for increasing integration times, the error in orthogonality for the $Q$-method increases. The corresponding error in orthogonality for the $e^S$-method remains within the machine precision of MATLAB ($\approx 2.2 \times 10^{-16}$) throughout the integration and at the scale shown on the plot it is practically zero.

The above numerical results for Duffing's equation show that in terms of the error in the sum of the LCEs and the error in orthogonality, the $e^S$-method is superior to the $Q$-method.

## 6. The 3D case

In this part of the paper we deal with the 3D case. Again, several dynamical systems can be decomposed to 3D systems for the purpose of computing LCEs. The differential equations that determine the elements of the skew symmetric matrix $S$ of the $e^S$-method are given, together with the differential equations that determine the LCEs. Computational results for the $e^S$-method are compared with those for the $Q$-method using the Lorenz system. For the case of the $Q$-method it will be shown that when using a fixed step-size fourth-order Runge–Kutta method, the method fails to compute the LCEs due to an

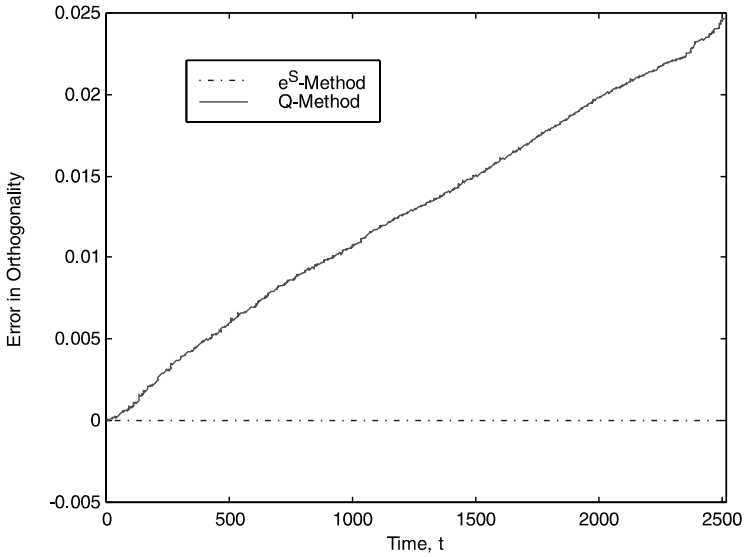


Fig. 13. Error in orthogonality $\|Q^{\mathrm{T}}Q - I\|_2$ for the $Q$- and the $e^S$-method.

overflow (or underflow) in the computations for all the chosen step-sizes, provided that sufficiently large integration times are used.

### 6.1. Equations to determine $S$ in the 3D case using the $e^s$-method

The derivation follows along the same lines as the derivation for the 2D case. Let $S$ be the skew-symmetric matrix such the $Q = e^S$, and let it be given by

$$S = \begin{bmatrix} 0 & -a(t) & -b(t) \\ a(t) & 0 & -c(t) \\ b(t) & c(t) & 0 \end{bmatrix}. \tag{73}$$

The eigenvalues of $S$ are $\mu_1 = 0$ and $\mu_{2,3} = \pm\sqrt{a(t)^2 + b(t)^2 + c(t)^2}\,i = \pm\mu i$. Using the eigenvalues of $S$, the matrix $e^S$ can be expressed as

$$\begin{aligned} e^S &= I + \frac{\sin(\mu)}{\mu}S + \frac{1-\cos(\mu)}{\mu^2}S^2 \\ &= \frac{1}{\mu^2}\begin{bmatrix} c^2 + (a^2+b^2)\cos(\mu) & -a\mu\sin(\mu) - bc(1-\cos(\mu)) & -b\mu\sin(\mu) + ac(1-\cos(\mu)) \\ a\mu\sin(\mu) - bc(1-\cos(\mu)) & b^2 + (a^2+c^2)\cos(\mu) & -c\mu\sin(\mu) - ab(1-\cos(\mu)) \\ b\mu\sin(\mu) + ac(1-\cos(\mu)) & c\mu\sin(\mu) - ab(1-\cos(\mu)) & a^2 + (b^2+c^2)\cos(\mu) \end{bmatrix}. \end{aligned} \tag{74}$$

Following the same procedure as for the 2D case, we use the observation that the product $e^{-S}(de^S/dt)$ is skew symmetric and $\dot{R}R^{-1}$ is upper triangular. The equations for $\dot{S}$ can thus be obtained by expanding the lower triangular part of

$e^{-S}(de^S/dt)$ and equating it to the lower triangular part of $e^{-S}Je^S$. In order to simplify some of the notation, recall that $e^S = Q$, thus $(e^{-S}Je^S)_{(i,j)} = q_i^T J q_j$, where $q_k$ is the $k$th column of $Q$. Note that from Eq. (74) we have an explicit expression for $Q$ in terms of the elements of $S$. With the last observations, and after some algebra, the differential equations for the elements of $\dot{S}$ are obtained as

$$A(t)\begin{bmatrix}\dot{a}(t)\\ \dot{b}(t)\\ \dot{c}(t)\end{bmatrix} = \begin{bmatrix}q_2^T J q_1\\ q_3^T J q_1\\ q_3^T J q_2\end{bmatrix}, \tag{75}$$

where the coefficient matrix $A(t)$is given by

$$A(t) = \frac{1}{\mu^3}\begin{bmatrix}\mu a^2 + (\mu^2 - a^2)\sin(\mu) & \mu(ab + c - c\cos(\mu)) - ab\sin(\mu) & \mu(ac - b + b\cos(\mu)) - ac\sin(\mu)\\ \mu(ab - c + c\cos(\mu)) - ab\sin(\mu) & \mu b^2 + (\mu^2 - b^2)\sin(\mu) & \mu(bc + a - a\cos(\mu)) - bc\sin(\mu)\\ \mu(ac + b - b\cos(\mu)) - ac\sin(\mu) & \mu(bc - a + a\cos(\mu)) - bc\sin(\mu) & \mu c^2 + (\mu^2 - c^2)\sin(\mu)\end{bmatrix}. \tag{76}$$

Inverting the matrix $A(t)$ ( $A^{-1}(t) = B(t)$) in (76), (75) becomes

$$\begin{bmatrix}\dot{a}(t)\\ \dot{b}(t)\\ \dot{c}(t)\end{bmatrix} = B(t)\begin{bmatrix}q_2^T J q_1\\ q_3^T J q_1\\ q_3^T J q_2\end{bmatrix}, \quad \text{and} \quad \begin{bmatrix}a(0)\\ b(0)\\ c(0)\end{bmatrix} = \begin{bmatrix}0\\ 0\\ 0\end{bmatrix}, \tag{77}$$

where the matrix $B(t)$ is

$$B(t) = \frac{1}{2\mu^2}\begin{bmatrix}\mu(\mu^2 - a^2)\cot\left(\frac{\mu}{2}\right) + 2a^2 & -ab\mu\cot\left(\frac{\mu}{2}\right) + 2ab - c\mu^2 & -ac\mu\cot\left(\frac{\mu}{2}\right) + 2ac + b\mu^2\\ -ab\mu\cot\left(\frac{\mu}{2}\right) + 2ab + c\mu^2 & \mu(\mu^2 - b^2)\cot\left(\frac{\mu}{2}\right) + 2b^2 & -bc\mu\cot\left(\frac{\mu}{2}\right) + 2bc - a\mu^2\\ -ac\mu\cot\left(\frac{\mu}{2}\right) + 2ac - b\mu^2 & -bc\mu\cot\left(\frac{\mu}{2}\right) + 2bc + a\mu^2 & \mu(\mu^2 - c^2)\cot\left(\frac{\mu}{2}\right) + 2c^2\end{bmatrix}. \tag{78}$$

In order to determine the LCEs we also need to solve the initial value problem

$$\begin{bmatrix}\dot{\rho}_1\\ \dot{\rho}_2\\ \dot{\rho}_3\end{bmatrix} = \begin{bmatrix}q_1^T J q_1\\ q_2^T J q_2\\ q_3^T J q_3\end{bmatrix}, \quad \text{and} \quad \begin{bmatrix}\rho_1(0)\\ \rho_2(0)\\ \rho_3(0)\end{bmatrix} = \begin{bmatrix}0\\ 0\\ 0\end{bmatrix}. \tag{79}$$

Eq. (77) gives the system of differential equations that determine the elements of $S$. We note that the right-hand side of (77) is only a function of the elements of $S$ and the Jacobian matrix. Similarly, the right hand side of Eq. (79) is only a function of the elements of $S$ and the Jacobian matrix.

In order to compute the LCEs we need to solve the initial value problems given in (1), (77) and (79), and the LCEs are then simply given by

$$\lambda_i = \lim_{t\to\infty}\frac{\rho_i(t)}{t} = \lim_{t\to\infty}\lambda_i(t) \quad \text{for } i = 1, 2, \text{ and } 3.$$

It should be noted that when $\mu = 2n\pi$, for $n = 0, 1, 2, 3, \ldots$, the matrix $A(t)$ given in Eq. (76) is singular, and $B(t)$ given in (78) is not defined. Thus for the above values of $\mu$ the differential equations for $\dot{a}$, $\dot{b}$ and $\dot{c}$ as given in Eq. (77) are not defined. For $\mu = 0$, we have that $S = 0$ and $e^S = I$, differentiating (74) and using (11), yields $\dot{a} = J_{21}$, $\dot{b} = J_{31}$ and $\dot{c} = J_{32}$. When the same method to obtain $\dot{a}$, $\dot{b}$ and $\dot{c}$ is applied to $\mu = 2n\pi$ for $n = 1, 2, 3, \ldots$, no explicit expressions for $\dot{a}$, $\dot{b}$ and $\dot{c}$ are obtained. However, one can avert this difficulty by simply changing to a different coordinate system in which the sought for quantities are then defined.

### 6.2. Numerical comparison between the $Q$- and $e^S$-methods the for the 3D case

A comparison of the accuracy of the $Q$- and the $e^S$-methods for computing the LCEs of 3D systems is performed in this section. A Lorenz system is used for the comparison. The numerical results presented in this section strongly suggest the superiority of the $e^S$-method over the $Q$-method. We show that the direct computational implementation of the $Q$-method without any effort to deal with the issue of the deviation from orthogonality can actually lead to a complete failure of the method.

Consider the Lorenz system given by

$$\begin{bmatrix} \dot{y}_1 \\ \dot{y}_2 \\ \dot{y}_3 \end{bmatrix} = \begin{bmatrix} \sigma(y_2 - y_1) \\ \rho y_1 - y_1 y_3 - y_2 \\ y_1 y_2 - \beta y_3 \end{bmatrix} \quad \text{and} \quad \begin{bmatrix} y_1(0) \\ y_2(0) \\ y_3(0) \end{bmatrix} = \begin{bmatrix} 0 \\ 1 \\ 0 \end{bmatrix}. \tag{80}$$

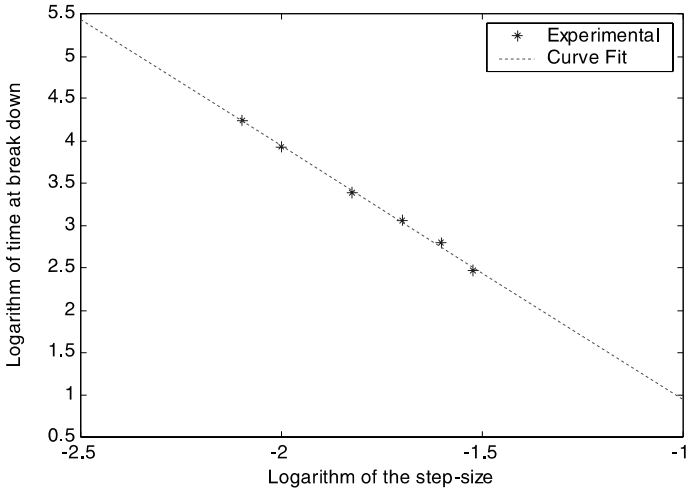


Fig. 14. Logarithm of the time when the $Q$-method fails versus the logarithm of the step size, $\Delta t$.

For the parameter values $\sigma = 16$, $\beta = 4$ and $\rho = 45.92$, the $Q$-method was implemented using a fixed time-step size ($\Delta t$), 4th order Runge–Kutta scheme. The LCEs were computed for different integration time-step sizes. For all the time-step sizes considered, the $Q$-method eventually failed, provided the integration was taken over a long enough time interval.

Fig. 14 shows the logarithm (base 10) of the time at which the $Q$-method failed in the computation of the LCEs vs. the logarithm of the size of the integration time-step. The results from numerical simulations are recorded as experimental points. Each time this failure was caused by an overflow (or underflow) which occurred in the computation of the orthogonal matrix $Q$. The curve fit plot corresponds to the least squares fit of the experimental points. The empirical equation resulting from the curve fit is *time to fail* $\approx 0.0087(\Delta t)^{-3.00}$. Thus as one would generally expect, the time it takes for the method to fail significantly decreases as the time step increases.

The following numerical results correspond to the computation of the LCEs using the $Q$-method with $\Delta t = 0.03$. The computed LCEs are shown in Fig. 15. The values are only shown up until the time when their growth would require a drastic change of the scale for their presentation on this plot.

The severe loss of orthogonality and the subsequent failure of the $Q$-method is illustrated in Fig. 16. The figure shows the error in orthogonality $\|Q^{\mathrm{T}}(t)Q(t) - I\|_2$ as a function of time when computing the LCEs using the $Q$-method with $\Delta t = 0.03$. For comparison, the figure also includes the error in orthogonality for the $e^S$-method when using the same fixed time-step size.

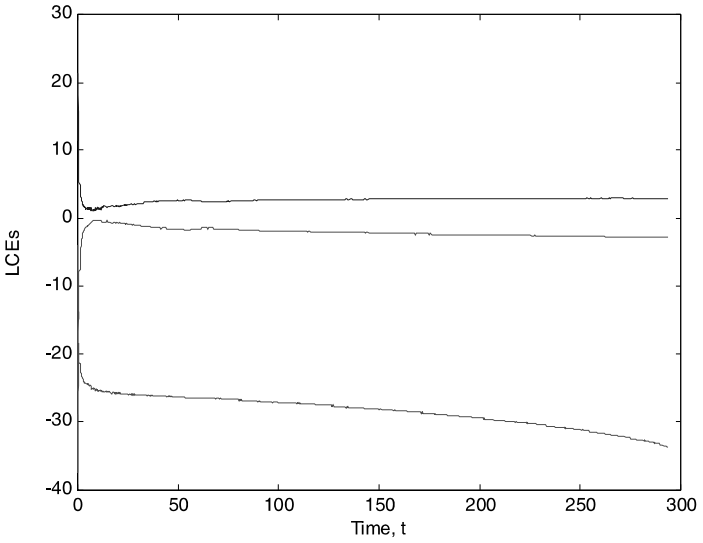


Fig. 15. Computed LCEs as a function of time, using the $Q$-method for the Lorenz system.

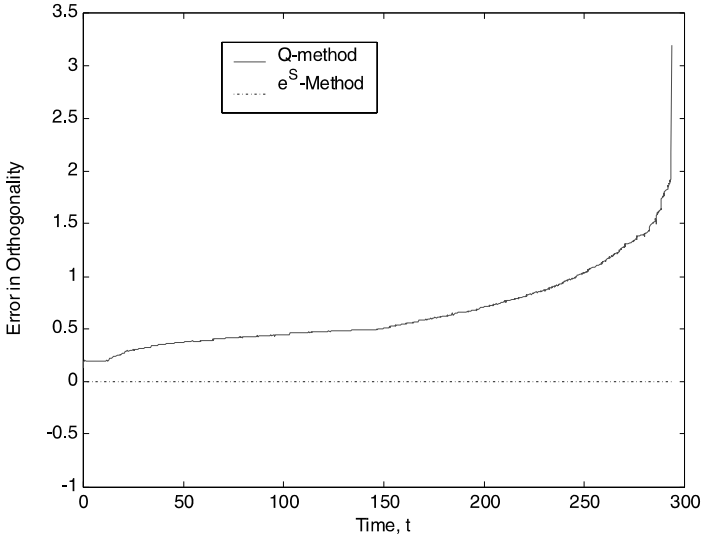


Fig. 16. Error in orthogonality for the $Q$- and the $e^S$-methods using the Lorenz system.

Since the trace of the Jacobian of the Lorenz system is a constant, then the sum of the time evolving LCEs is the constant trace. For the Lorenz system we then have $\lambda_1 + \lambda_2 + \lambda_3 = -\sigma - \beta - 1$, thus for the parameters $\sigma = 16$ and $\beta = 4$ used in the example we have $\lambda_1 + \lambda_2 + \lambda_3 = -21$. Fig. 17 shows the error in the sum of the LCEs (i.e., $\lambda_1 + \lambda_2 + \lambda_3 + 21$) of the Lorenz system (80) as a function of time when the $Q$- and $e^S$-methods were used with a fixed integration time-step size of $\Delta t = 0.03$. From the plot, we see that as time increases the error in the sum for the $Q$-method deviates further and further from the theoretical value of 0. On the other hand, the error in the sum of the LCEs for the $e^S$-method is practically zero at the scale of the plot shown.

The above example illustrates that the direct implementation of the $Q$-method to compute the LCEs may not just provide erroneous, and numerically inaccurate results; it can actually break down due to numerical overflows and/or underflows when carried along far enough in time (note, our aim is to obtain $\lambda_i(t)$ as $t \to \infty$).

The following numerical results correspond to the $e^S$-method when implemented to solve the above mentioned Lorenz system. For purposes of comparison, a fixed time-step size, fourth-order, Runge–Kutta integrator was used with $\Delta t = 0.03$, as in the $Q$-method. The $e^S$-method did not encounter any numerical overflows as did the $Q$-method for any of the integration final times that we considered. For illustrative purposes we present the numerical results over a time interval of 1000 units. The computed LCEs for $\Delta t = 0.03$ were 1.5792, −0.1311 and −22.4481 at time $t = 1000$. Fig. 18 shows a plot of the

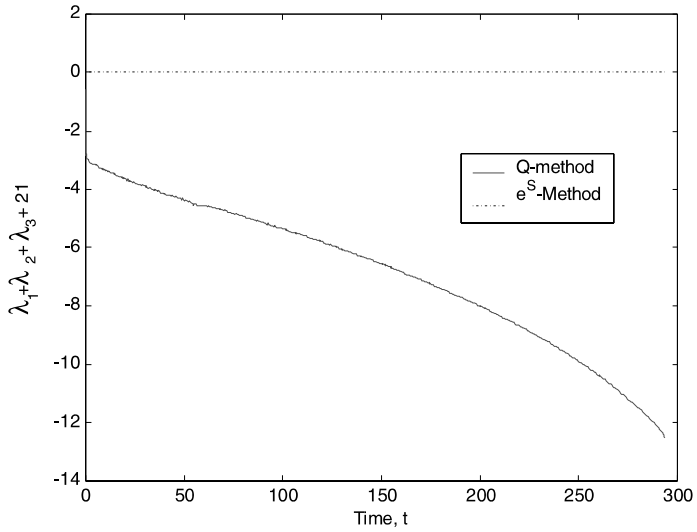


Fig. 17. Sum of the computed LCEs versus time using the $Q$- and the $e^S$-methods.

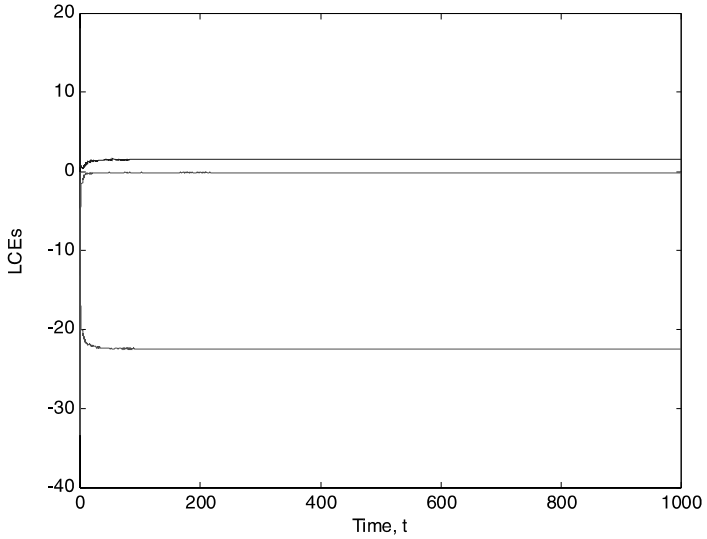


Fig. 18. Computed LCEs as a function of time, using the $e^S$-method for the Lorenz system over at time interval of 1000.

computed LCEs as a function of time. To the scale of the plot, the LCEs seem to be clearly converging to finite values around $t = 300$. In contrast, the computed LCEs using the $Q$-method as shown on Fig. 15 do not appear to be converging towards finite values, in particular the smallest LCE. Note that here $\Delta t = 0.03$ was used only for making comparisons with results obtained using the $Q$-method; for more accurate estimates of the LCEs of the system (80), a smaller time-step size would be preferable. Using $\Delta t = 0.001$ $t = 1,000$ the $e^S$-method gives the LCEs: $\lambda_1 = 1.4898$; $\lambda_2 = 0.0048$ and $\lambda_3 = -22.4946$. Theoretically, the Lorenz system has one zero LCE; observe that $\lambda_2$ is close to zero, validating the numerical results.

Fig. 19 shows the error in orthogonality ($\|Q^{\mathrm{T}}(t)Q(t) - I\|_2$) for the $e^S$-method. The method yields almost orthogonal matrices with error in orthogonality of order $10^{-15}$ throughout the entire time interval of integration.

Fig. 20 shows that the error in the sum of the LCEs for the $e^S$-method is of the order of $10^{-11}$. In contrast, for the much smaller interval in time for which the $Q$-method still 'functions', the error in the sum of the LCEs is of the order of 10 (see Fig. 17).

When comparing the numerical efficiency of the $e^S$ and the $Q$-methods, the ratio of the number of flops required over one integration time-step of the $e^S$-method to the $Q$-method is about 0.9. Perhaps one would expect larger computational savings when using the $e^S$-method since after all, one only needs

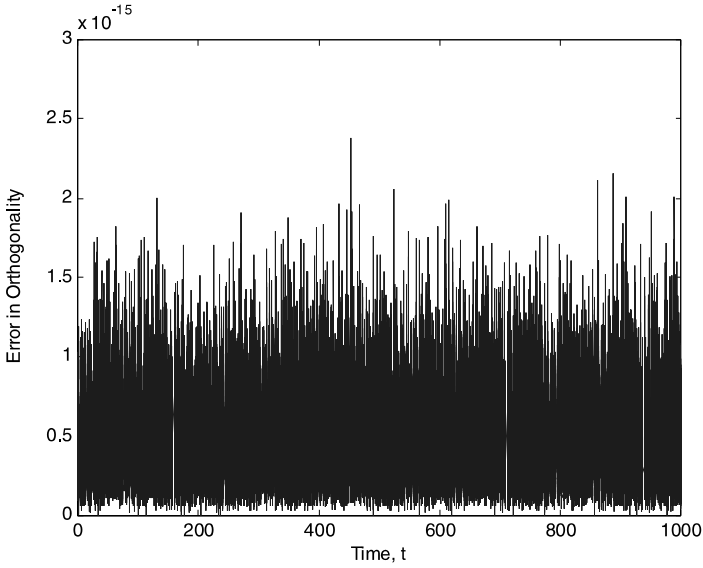


Fig. 19. Error in orthogonality for the $e^S$-method as a function of time for the Lorenz system over a time interval of 1000.

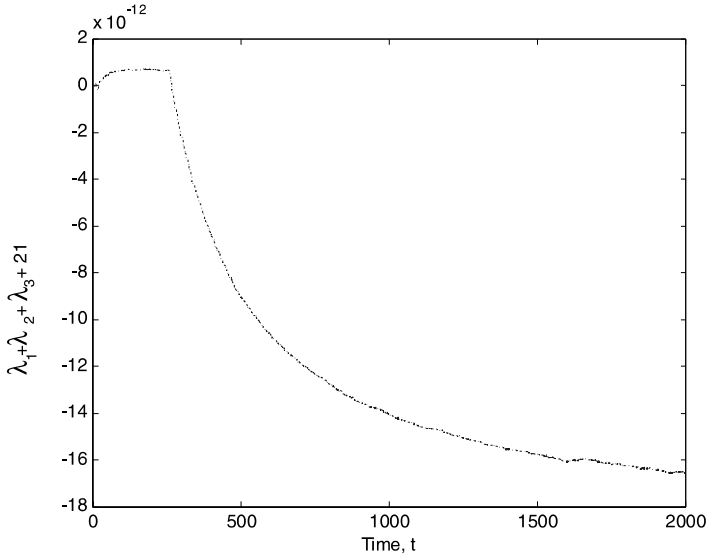


Fig. 20. Error in the sum of the computed LCEs versus time using the $e^S$-method for the Lorenz system over a time interval of 2000.

to solve three differential equations to get $Q$ versus nine when using the $Q$-method. The added computation cost in the $e^S$-method comes from the fact that $Q$ needs to be reconstructed from $S$.

## 7. Conclusions

In this paper we have presented a method to compute the LCEs for continuous dynamical systems which is accurate and more efficient than the methods generally used in the literature. The most prevalent method for computing LCEs is shown to be prone to breakdown. In this paper a new method is proposed which avoids this problem and in addition computes the LCEs in an efficient and accurate manner.

In general the methods to compute the LCEs of dynamical systems involve either a $QR$-factorization or a singular value factorization of the fundamental solution. The method presented in this paper focuses on the $QR$-factorization and it is based on the observation that any orthogonal matrix $Q$ with $\det(Q) = 1$ can be expressed as the exponential of a skew symmetric matrix $S$, i.e., $Q = e^S$. In our method we determine the differential equations that establish $S$, and thus by construction, the matrix $Q = e^S$ is orthogonal. The accuracy of the computed LCEs is generally affected by the orthogonality of $Q$. Since the new method guarantees the orthogonality of $Q$, the new approach is

expected to be highly accurate since errors due to errors in orthogonality are virtually absent. The fact that the orthogonality of $Q$ is preserved also assures that the method will not fail due to any overflows (or underflows) in the computations. The representation of $Q$ in terms of the elements of $S$ allows us to determine $S$ (and thus $Q$) by using only $n(n-1)/2$ differential equations. In contrast, the methods that attempt to find $Q$ directly involve $n^2$ differential equations. The computational advantage (in terms of the number of differential equations needed to be solved to find $Q$) of the $e^S$-method over the $Q$-method is then given by the factor $\gamma = 2/(1-1/n)$. Thus for large $n$, the $e^S$-method is about twice more computationally advantageous than the $Q$-method. However this ratio may not portray the exact computational advantage of the $e^S$-method since we require the $Q$ matrix to be reconstructed from $S$.

The proposed approach is used for continuous dynamical systems of two and three dimensions; these constitute by far the most numerous types of systems studied to date in the literature. Furthermore, many dynamical systems can be broken down, for purposes of computing the LCEs, into 2D and/or 3D blocks, as illustrated in Section 5.3, and more generally, in Appendix A. The differential equations needed to compute the LCEs in terms of the elements of $S$ and the Jacobian matrix for these systems are given. For the 2D case with constant Jacobian, closed form expressions for the time evolution of the LCEs are given in terms of the elements of the Jacobian. The numerical examples comparing the proposed approach and the standard method for 2 and 3D systems show the superiority of the $e^S$-method over the $Q$-method.

Adaptations of the $e^S$-method to systems of dimension four and five appear possible. However, systems of higher dimension may require the use of specialized tools from Lie algebra. Yet, there are many physical systems described by differential equations of higher order ($n > 3$) which can be decomposed for the purposes of computing LCEs into smaller subsystems, depending of the structure of the Jacobian matrix. When such decomposition into 2 and 3D subsystems is possible, the methods in this paper can be directly applied.

## Appendix A

Three results are presented in this appendix.

1. The first result states that when the Jacobian $J$ of (2) has a block upper triangular structure (i.e., it has square matrices along the diagonal with zeros in all entries below its block diagonal structure and where the elements above the diagonal blocks need not be zero), then the solution $Y$ of (2) has the same structure. This implies that the $QR$-decomposition of $Y$ yields a matrix $Q$ with special structure that allows us to decompose the problem of finding the LCEs into two sub-problems, each with its own $QR$-decomposition. We then prove an important corollary when the Jacobian has an upper-tri-

angular (not just block upper triangular) structure and show how in that circumstance the orthogonal factorization of the system is trivial. Such special upper-triangular structures are often found in dynamical models of physical systems.
2. The second result shows that for systems which have a block upper triangular structure (as in Result 1), the LCEs can be determined by considering smaller subsystems. From this follows an important corollary, when the Jacobian matrix is upper triangular; then the LCEs can be found trivially.
3. The third result shows that at each instant of time, the sum of the time evolving LCEs is equal to the time average of the trace of the Jacobian matrix of the system. This is a generalization of a result which is often found in various restricted forms, such as those dealing with constant Jacobian matrices, and/or with the sum of the final computed LCEs of a dynamical system.

**Result A.1.** Suppose that the $n$ by $n$ Jacobian, $J$, of (2) has the following block upper triangular structure

$$J = \begin{bmatrix} J_1 & J_2 \\ O & J_3 \end{bmatrix}, \tag{A.1}$$

where $J_1$ is $m$ by $m$, $J_2$ is $m$ by $p$, $J_3$ is a $p$ by $p$ matrix and $O$ is a $p$ by $m$ zero matrix, with $m + p = n$.

Then the solution $Y$ of the initial value problem (2) has the same structure as $J$ and it has a $QR$-decomposition

$$Y = \begin{bmatrix} Y_1 & Y_2 \\ O & Y_3 \end{bmatrix} = \begin{bmatrix} Q_1 & \tilde{O} \\ O & Q_3 \end{bmatrix} \begin{bmatrix} R_1 & R_2 \\ O & R_3 \end{bmatrix}, \tag{A.2}$$

where, $Y_1$, $R_1$ and $Q_1$ are $m$ by $m$ matrices, with $R_1$ upper triangular, and $Q_1$ orthogonal; $Y_2$, $R_2$ and $\tilde{O}$ are $m$ by $p$ matrices, with $\tilde{O}$ a zero matrix; $Y_3$, $R_3$ and $Q_3$ are $p$ by $p$ matrices, with $R_3$ upper triangular, $Q_3$ orthogonal; and $O$ is a $p$ by $m$ zero matrix. Thus we obtain the two $QR$-decompositions $Y_1 = Q_1 R_1$ and $Y_3 = Q_3 R_3$.

**Proof.** First we show that if $J$ has the structure given in (A.1), then $Y$ has the same structure. Consider the initial value problem (2), and consider a candidate solution $Z$ with

$$Z = \begin{bmatrix} Z_1 & Z_2 \\ O & Z_3 \end{bmatrix}, \tag{A.3}$$

where $Z_1$ is $m$ by $m$, $Z_2$ is $m$ by $p$, $Z_3$ is a $p$ by $p$ matrix, and $O$ is a $p$ by $m$ zero matrix. The structure of $\dot{Z}$ is the same as the structure of $Z$, and since the

product $JZ$ has the same structure as $Z$, the structure of $Z$ given by (A.3) satisfies (2). Furthermore, since at $t = 0$, $Y = I$, the structure of $Z$ also satisfies the initial conditions of (2). Therefore the structure of the candidate solution is correct and by the uniqueness of the solution of (2), the solution $Y$ has the same structure as $Z$, which in turn is the same as that of $J$.

$Y$ is non-singular for all time, since it is a fundamental solution satisfying nonsingular initial conditions. Thus, $Y$ has a unique $QR$-decomposition with a non-singular upper triangular $R$ matrix all of whose diagonal elements are positive. We can then write the $QR$-decomposition of $Y$ in matrix block form as

$$\begin{bmatrix} Y_1 & Y_2 \\ O & Y_3 \end{bmatrix} = \begin{bmatrix} Q_1 & Q_2 \\ Q_4 & Q_3 \end{bmatrix} \begin{bmatrix} R_1 & R_2 \\ O & R_3 \end{bmatrix} = \begin{bmatrix} Q_1R_1 & Q_1R_2 + Q_2R_3 \\ Q_4R_1 & Q_4R_2 + Q_3R_3 \end{bmatrix}, \tag{A.4}$$

where the elements of $Y$ and $R$ have the same shape and dimensions as given in (A.2), and the blocks, forming $Q$ have the appropriate dimensions.

Equating the zero matrix $O$ from the left-hand side of (A.4) with the corresponding entries of the right-hand side of (A.4) yields $O = Q_4R_1$. Since $R_1$ is non-singular, $Q_4 = O$. Since $Q_4 = O$ we have that $Y_3 = Q_3R_3$. Since the last $p$ rows of $Q$ are orthogonal, $Q_3$ is orthogonal. Thus $Y_3 = Q_3R_3$ is a $QR$-factorization of $Y_3$. Since $Q_3$ is orthogonal and the last $p$ columns of $Q$ are of unit length, $Q_2 = O$. Thus the $QR$-decomposition of $Y$ is as given in (A.2). □

**Remark A.1.** The above result implies that in order to obtain the partial $QR$-factorization of $Y$ (i.e., when the matrix $R_2$ is not needed, as is the case when determining the LCEs), one only has to find the $QR$-decompositions of the subsystems $Y_1 = Q_1R_1$ and $Y_3 = Q_3R_3$. It is clear that the same argument used above holds for systems with Jacobian matrices that have block upper triangular structure with say $k$ blocks along the diagonal. And that in order to determine the partial $QR$-factorization of $Y$ (i.e., excluding the off diagonal blocks of $R$), one only needs to consider the appropriate $k$ subsystems.

**Corollary A.1.** *If in the initial value problem given by* (2), *the Jacobian matrix J is an upper triangular matrix*, *then Y is upper triangular*, *and the unique QR-factorization* $Y = QR$, (*where the diagonal elements of R are positive*) *is such that* $Q = I$ (*the identity matrix*).

**Proof.** Following the same reasoning as before it is easy to show that the solution $Y$ of (2) has the same structure as $J$ (i.e., upper triangular). Since $Y$ and $R$ are upper triangular, then in general the unique orthogonal matrix $Q$ of the decomposition of $Y$ which yields positive diagonal elements of $R$ would be a diagonal matrix with either $\pm 1$ along the diagonal elements. Also, at

$t = 0$, $Y = I$, so that $Q = I$ and $R = I$. Furthermore, $Y$ is nonsingular for all time. A unique decomposition $Y(t) = Q(t)R(t)$ at any time $t$ can be done where the diagonal elements of $R(t)$ are all positive. Now if an element along the diagonal of $Q(t)$ (which starts out at $t = 0$ as $I$) changes sign at time $t$, the corresponding diagonal element of $Y(t)$ must change sign (since $Y = QR$). Because of continuous dependence, that element of $Y$ must then pass through zero at some time $0 < \tau < t$. But this is not possible, for then $Y$ would become singular at time $\tau$. Hence no element of $Q$ can change sign. Therefore, $Q(t) = I$. □

**Result A.2.** Suppose that the $n$ by $n$ Jacobian, $J$, of (2) has the block upper triangular structure given in (A.1). Then in order to determine the LCEs of the system one only needs to consider the uncoupled subsystems

$$\dot{Y}_1 = J_1 Y_1, \quad Y_1(0) = I, \tag{A.5}$$

$$\dot{Y}_3 = J_3 Y_3, \quad Y_3(0) = I, \tag{A.6}$$

with $J_1$ and $J_3$ as in (A.1), and $Y_1$ and $Y_3$ as in (A.2).

**Proof.** From Result 1 we have that the $QR$-factorization of $Y$ is given by (A.2). In order to obtain the LCEs of the system, we only need the diagonal elements of $R_1$ and $R_3$. These diagonal elements can be found by considering the $QR$-factorizations of $Y_1$ and $Y_3$ which are dictated by the initial value problems (A.5) and (A.6). □

**Corollary A.2.** *If in the initial value problem given by* (2), *the n by n Jacobian matrix J is an upper triangular matrix, then the LCEs of the system can be obtained by solving*

$$\dot{\rho}_i = \frac{\dot{R}_{ii}}{R_{ii}} = J_{ii}, \ \rho_i(0) = 0 \quad \textit{for } i = 1, \ldots, n. \tag{A.7}$$

*The LCEs,* $\lambda_i = \lim_{t\to\infty} \frac{\rho_i(t)}{t} = \lim_{t\to\infty} \lambda_i(t)$, *are then determined by quadrature as*

$$\lambda_i(t) = \frac{1}{t} \int_0^t (J(\tau))_{ii} d\tau, \quad \textit{for } i = 1, \ldots, n. \tag{A.8}$$

**Proof.** The corollary follows trivially from Corollary 1. The orthogonal matrix $Q$ of the $QR$-decomposition of $Y$ (the solution of (2)) is simply the constant matrix $Q = I$. By Eq. (8) we then have that

$$\dot{\rho}_i = \frac{\dot{R}_{ii}}{R_{ii}} = J_{ii}, \rho_i(0) = 0 \quad \text{for } i = 1, \ldots, n. \tag{A.9}$$

By directly integrating each Eq. (A.8) we then get Eq. (A.7)

$$\lambda_i = \lim_{t\to\infty} \frac{\rho_i(t)}{t} = \lim_{t\to\infty} \lambda_i(t),$$
$$\text{where } \lambda_i(t) = \frac{1}{t}\int_0^t (J(\tau))_{ii}\, \mathrm{d}\tau \quad \text{for } i = 1,\ldots,n. \qquad \square$$

**Remark A.2.** Result 2 clearly generalizes to systems that have block upper triangular Jacobian matrices. That is, if the block upper triangular Jacobian matrix $J$ has say $k$ blocks along the diagonal, then one only needs to consider $k$ subsystems in order to find the LCEs. Further simplifications are possible if any of the $k$ diagonal blocks of $J$ are upper triangular. For any such block, the results from Corollary 2 hold, reducing the determination of the LCEs for those blocks to simple quadratures.

**Result A.3.** At each instant of time, the sum of the time evolving LCEs is equal to the time average of the trace of the Jacobian, that is

$$\sum_{i=1}^{n} \lambda_i(t) = \frac{\ln\left(\prod_{i=1}^{n} R_{ii}(t)\right)}{t} = \frac{1}{t}\int_0^t \text{Trace}\,(J(\tau))\,\mathrm{d}\tau. \tag{A.10}$$

**Proof.** The Jacobi–Liouville [5] relation applied to (2) gives

$$\det(Y(x;t)) = \exp\left(\int_0^t \text{Trace}\,(J(\tau))\mathrm{d}\tau\right) = \det(Q(t)R(t)), \tag{A.11}$$

where the second equality follows from the $QR$-decomposition, $Y = QR$. The matrix $Q$ is orthogonal. Since $Y(0) = Q(0) = I_n$ and the solution of (2) is nonsingular, $\det(Q(t)) = +1$. Noting that $R$ is upper triangular, taking logarithms, and dividing by $t$, yields the result. $\square$

## References

[1] A.M. Lyapunov, Problème Général de la Stabilité du Mouvement, Princeton University Press, Princeton, NJ, 1947 (report of the French translation in 1907 of the Russian memoire dated 1892).
[2] T. Parker, L. Chua, Practical Numerical Algorithms for Chaotic Systems, Springer, Berlin, 1989.
[3] C. Froeschle, E. Lega, R. Gonczi, Fast Lyapunov indicators-application to asteroidal motion, Celestial Mechanics and Dynamical Astronomy 1 (67) (1997) 41–62.
[4] G. Nicolis, D. Daems, Nonequilibrium thermodynamics of dynamical systems, J. Physical Chemistry 100 (49) (1996) 19187–19191.

[5] See [17] for a proof of the Jacobi–Liouville relation.

[5] G. Schmid, R. Dunkin, Indications of nonlinearity intraindividual specificity and stability of human EEG – The unfolding dimension, Physica D 93 (3-4) (1996) 165–190.
[6] V. Efimov, A. Prusov, M. Shokurov, Seasonal instability of pacific sea-surface-temperature anomalies, Quarterly J. Royal Meteorological Society Suppl. B 123 (538) (1997) 337–356.
[7] G. Benettin, L. Galgani, A. Giorgilli, J.M. Strelcyn, Lyapunov characteristic exponents for smooth dynamical systems and for hamiltonian systems; a method for computing all of them Part I & II, Meccanica 15 (1980) 9–30.
[8] G. Benettin, L. Galgani, A. Giorgilli, J.M. Strelcyn, Tous les nombres caractéristiques de Lyapunov sont effectivement calculables, Comptes Rendues Acad. Sc. Paris 286A (1978) 431–433.
[9] K. Geist, U. Parlitz, W. Lauterborn, Comparison of different methods for computing Lyapunov exponents, Prog. Theor. Phys. 83 (5) (1990) 875–893.
[10] L. Diecci, R. Russel, E. van Vleck, On the computation of Lyapunov exponents for continuous dynamical systems, SIAM J. Numer. Anal. 34 (1) (1997) 402–423.
[11] L. Diecci, E. van Vleck, Computation of a few Lyapunov exponents for continuous and discrete dynamical systems, Appl. Numer. Math. 17 (3) (1995) 275–291.
[12] H. von Bremen, F. Udwadia, W. Proskurowski, An efficient QR based method for the computation of Lyapunov exponents, Physica D 101 (1997) 1–16.
[13] F.R. Gantmacher, The Theory of Matrices, vol. 1, Chelsea, New York, NY, 1958.
[14] R.E. Bellman, R.E. Kalaba, in: Quasilinearization and Nonlinear Boundary-Value Problems, Elsevier, New York, 1965.
[15] F.C. Moon, in: Chaotic Vibrations: An Introduction for Applied Scientists and Engineers, Wiley, New York, 1987.
[16] Y. Ueda, Random transitional phenomena in the system governed by Duffing's equation, J. Statist. Phys. 20 (2) (1979) 181–196.
[17] E.A. Coddington, N. Levinson, Theory of Ordinary Differential Equations, Reprint edition, Krieger, Malabar, FL, 1984.